

AD-A042 666

NORTHROP CORP DES PLAINES ILL  
LOW COST CROSSED-FIELD AMPLIFIER. (U)  
JUN 77 R R MOATS

F/G 9/1

UNCLASSIFIED

094-007824

ECOM-75-1343-F

DAAB07-75-C-1343  
NL

| OF |

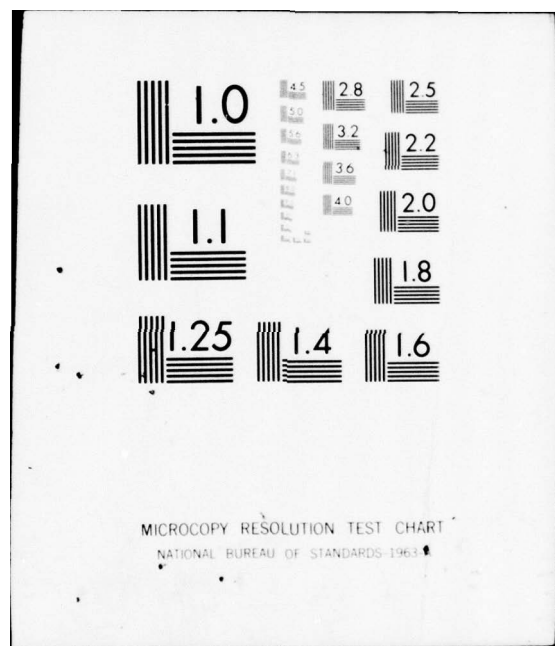
ADA042-666



END  
DATE  
FILMED

8 - 77

DDC





(12)

g

AD A 042666

Research and Development Technical Report

ECOM -75-1343-F

LOW COST CROSSED-FIELD AMPLIFIER

R. R. Moats  
Northrop Corporation  
175 W. Oakton Street  
Des Plaines, IL 60018

June 1977

Final Technical Report

DISTRIBUTION STATEMENT

Approved for public release;  
distribution unlimited.

Prepared for:

**ECOM**

US ARMY ELECTRONICS COMMAND FORT MONMOUTH, NEW JERSEY 07703

DDC  
APR 9, 1977  
C

ADJ NO. \_\_\_\_\_  
DDC FILE COPY

## NOTICES

### Disclaimers

The findings in this report are not to be construed as an official Department of the Army position, unless so designated by other authorized documents.

The citation of trade names and names of manufacturers in this report is not to be construed as official Government indorsement or approval of commercial products or services referenced herein.

### Disposition

Destroy this report when it is no longer needed. Do not return it to the originator.

UNCLASSIFIED

SECURITY CLASSIFICATION OF THIS PAGE (When Data Entered)

19 REPORT DOCUMENTATION PAGE		READ INSTRUCTIONS BEFORE COMPLETING FORM
1. REPORT NUMBER ECOM 75-1343-F	2. GOVT ACCESSION NO.	3. RECIPIENT'S CATALOG NUMBER
4. TITLE (and Subtitle) Low Cost Crossed-Field Amplifier	5. TYPE OF REPORT & PERIOD COVERED Final Technical Report	
7. AUTHOR(s) R. R. Moats	6. PERFORMING ORG. REPORT NUMBER 094-007824	8. CONTRACT OR GRANT NUMBER(s) DAAB07-75-C-1343
9. PERFORMING ORGANIZATION NAME AND ADDRESS Northrop Corporation 175 East Oakton Street Des Plaines, Illinois 60018	10. PROGRAM ELEMENT, PROJECT, TASK AREA & WORK UNIT NUMBERS 1S762705AH94-B1-08	
11. CONTROLLING OFFICE NAME AND ADDRESS US Army Electronics Command ATTN: DRSEL-TL-BM Ft. Monmouth, New Jersey 07703	12. REPORT DATE June 1977	
14. MONITORING AGENCY NAME & ADDRESS (if different from Controlling Office) 1247p	13. NUMBER OF PAGES 49	
16. DISTRIBUTION STATEMENT (of this Report) Approved for public release Distribution Unlimited		15. SECURITY CLASS. (of this report) UNCLASSIFIED
17. DISTRIBUTION STATEMENT (of the abstract entered in Block 20, if different from Report)		
18. SUPPLEMENTARY NOTES		
19. KEY WORDS (Continue on reverse side if necessary and identify by block number) Electron Tubes, Microwave Amplifiers, Crossed-Field Tubes Shaped Substrate Meanderline		
20. ABSTRACT (Continue on reverse side if necessary and identify by block number) This work is directed toward the achievement of a lower cost slow-wave structure for an injected-beam crossed-field amplifier (IBCFA) than has heretofore been possible. For cost reduction, the meander type of structure is to be supported on an ECOM designed shaped-dielectric substrate instead of individual insulator bars. The slow-wave structure designed and built simulates the configuration of the shaped substrate,		

DD FORM 1 JAN 73 1473

EDITION OF 1 NOV 65 IS OBSOLETE

UNCLASSIFIED

SECURITY CLASSIFICATION OF THIS PAGE (When Data Entered)

409 790

UNCLASSIFIED

SECURITY CLASSIFICATION OF THIS PAGE(When Data Entered)

20. (cont'd)

but is built using conventional technology. In other respects, the design of the tube is similar to a production line IBCFA.

Performance of the first experimental model is considered, in general, representative of the capability of this design. Power output of more than 3 kW and over 30 percent efficiency was achieved in the middle of the 2-4 GHz band, measured with 20 dB gain. Performance in the lower half of the band degraded slowly as frequency was reduced below 2.6 GHz, and degraded more rapidly as frequency was increased above 3.4 GHz. Substantial power and efficiency increases were observed for increased drive, indicating that a longer interaction space is desirable. Efficiency levels not far different from those at 3 kW peak power output were observed at 1 kW, 2 kW and 4 kW peak power output by adjusting the magnetic field and the applied voltages.

A CFA built with a simulated flat-substrate meander line produced somewhat less power output and efficiency, and less bandwidth, both total (with sole tuning) and instantaneous. Power output up to 2.6 kW with normal rf drive and beam power (as above) was achieved, with operation from 2 to 3.6 GHz. Design corrections for improved performance are foreseen.

One of the experimental tubes was rebuilt with the Medicus nickel matrix cathode. Representative results were not achieved because of cathode contamination. However, results on another CFA show that successful use of such cathodes is likely in the CFA's of interest to ECOM.

UNCLASSIFIED

SECURITY CLASSIFICATION OF THIS PAGE(When Data Entered)

# TABLE OF CONTENTS

<u>Paragraph</u>		<u>Page</u>
1	INTRODUCTION . . . . .	1
2	SHAPED-SUBSTRATE MEANDER LINE . . . . .	3
	2.1 General Approach . . . . .	3
	2.2 Cold-Test Models . . . . .	7
	2.3 Electrical Design of Operating CFA . . . . .	13
	2.4 Operating Characteristics . . . . .	16
3	FLAT SUBSTRATE MEANDER LINE . . . . .	25
	3.1 General Approach . . . . .	25
	3.2 Cold-Test Model . . . . .	25
	3.3 Operating CFA with Simulated Flat Substrate . . . . .	27
4	MEDICUS NICKEL MATRIX CATHODE . . . . .	33
5	CONCLUSIONS . . . . .	37
6	RECOMMENDATIONS . . . . .	39
	BIBLIOGRAPHY . . . . .	41

ACCESSION for	
NRIS	W. Va. Section <input checked="" type="checkbox"/>
DDC	Bull. Section <input type="checkbox"/>
UNANNOUNCED	<input type="checkbox"/>
JUSTIFICATION	
BY	
DISTRIBUTION/AVAILABILITY CODES	
SPECIAL	
A	

# LIST OF ILLUSTRATIONS

<u>Figure</u>		<u>Page</u>
1	Shaped-Substrate on Line Support Block . . . . .	4
2	Ladder-Shaped Substrate with Meander Line . . . . .	4
3	Meander Line (Vane Configuration Indicated) . . . . .	5
4	Shaped-Substrate Meander Line: Multiple Insulators in Grooves . . . . .	6
5	Delay Ratio: Cold-Test Meander Lines for Low Cost CFA . . .	8
6	Coupling Impedance: Cold-Test Meander Line for Low Cost CFA . . . . .	10
7	Simulated Ladder-Substrate Meander Line: Multiple Insulators in Grooves . . . . .	11
8	Delay Ratio of Meander Line with Ladder-Substrate Compared with Meander Substrate . . . . .	12
9	(a) Initial Grid Design . . . . .	15
9	(b) Improved Grid Design with Openings Extended Over Edge Toward Interaction Space . . . . .	15
10	Delay Ratio of First CFA Model . . . . .	17
11	Power Output of IBCFA with Waveguide Load . . . . .	18
12	Power Output of IBCFA with Coaxial Load . . . . .	19
13	Power Output of IBCFA with Coaxial Load as a Function of RF Drive Power . . . . .	20
14	Spurious Signals in IBCFA (ECOM CFA No. 1) . . . . .	21
15	Power Output of IBCFA with Increased Beam Current (ECOM CFA No. 1) . . . . .	23
16	Meander Line with Increased Dielectric Loading . . . . .	26
17	Cross Section of Simulated Flat-Substrate Meander Line . . .	28
18	Power Output of Flat-Substrate IBCFA . . . . .	30
19	Transmission Loss in Simulated Flat-Substrate CFA Before and After Operation . . . . .	32
20	Medicus Type Nickel Matrix Cathode for CFA . . . . .	34

## LIST OF TABLES

<u>Table</u>		<u>Page</u>
1	Summary of Cold Test Models . . . . .	9
2	Low Cost CFA with Simulated Shaped Substrate Line: Specifications . . . . .	14
3	Low Cost CFA with Simulated Flat Substrate Line: Specifications . . . . .	29

## 1. INTRODUCTION

The research and development effort of this program was directed toward the ultimate achievement of a low-cost injected beam crossed-field amplifier (IBCFA). A major cost factor in present IBCFA's is the meander slow-wave structure, which incorporates a meander strip of copper and one separate ceramic insulator supporting each segment of the meander. By replacing the set of insulators with a single shaped-substrate which can be manufactured at moderate cost, very substantial cost savings in both time and labor can be achieved. An alternative approach, using a flat continuous substrate instead of a shaped-substrate, was also explored. Both the shaped-substrate and the flat-substrate concepts were originated by ECOM personnel, and have been the subject of a previous study by C. Bates and J. Hartley of ECOM. An additional area of study was the application of the Medicus type of nickel matrix cathode to the IBCFA's investigated here. Such cathodes represent a possible replacement for the relatively expensive tungsten matrix dispenser cathodes which have generally been used in IBCFA's.

The objective performance characteristics were as follows:

Frequency range	2 to 4 GHz
Peak power output	3 kW
Average power output	1 kW
Efficiency	35%
Gain	20 dB
Cathode voltage	7 kV (maximum)

These performance characteristics are in general quite similar to Northrop's RW-619.

A further objective was to design an IBCFA in which the condition for  $90^\circ$  phase drift per bar falls within the operation band. In the RW-619, it falls just above the operating band. Successful results with this frequency falling in the operating band lead to some significant advantages. The pitch of the line is greater so that construction is less difficult, and part tolerances are less stringent. Also, attenuation is less, thus increasing efficiency.

In addition, the line becomes wider so that cathode emission density, beam density, and thermal dissipation density are reduced, and the ultimate peak and average power capability is increased. Since it is expected that this technology will eventually be extended to I/J Band, these considerations become especially important.

The principal purpose of this program was to demonstrate the operational feasibility of the shaped-substrate and the flat-substrate meander line. To demonstrate feasibility, existing CFA technology was used insofar as possible, with the substrate configurations simulated by individual bars, instead of a one-piece shaped-substrate or a monolithic flat-substrate. The simulation of the shaped-substrate and flat-substrate in such a manner allowed the use of a large number of parts and sub-assemblies of proven design from production CFA's. The development of the new technology necessary for supporting single-piece ceramic substrates requires a major redesign of the total structure.

A CFA built with a simulated shaped-substrate meander line demonstrated excellent power and efficiency over an octave band. Peak power was over 3 kW over much of the band with normal rf drive (30-40W) and beam power (10.5 kW). Power output up to 3.8 kW was achieved with increased rf drive. Efficient operation for 1, 2, and 4 kW outputs was also demonstrated with adjustment of operating parameters.

A CFA built with a simulated flat-substrate meander line produced somewhat less power output and efficiency, and less bandwidth, both total (with sole tuning) and instantaneous. Power output up to 2.6 kW with normal rf drive and beam power (as above) was achieved, with operation from 2 to 3.6 GHz. Design corrections for improved performance are foreseen.

One of the experimental tubes was rebuilt with the Medicus nickel matrix cathode. Representative results were not achieved because of cathode contamination. However, results on another CFA show that successful use of such cathodes is likely in the CFA's of interest to ECOM.

## 2. SHAPED-SUBSTRATE MEANDER LINE

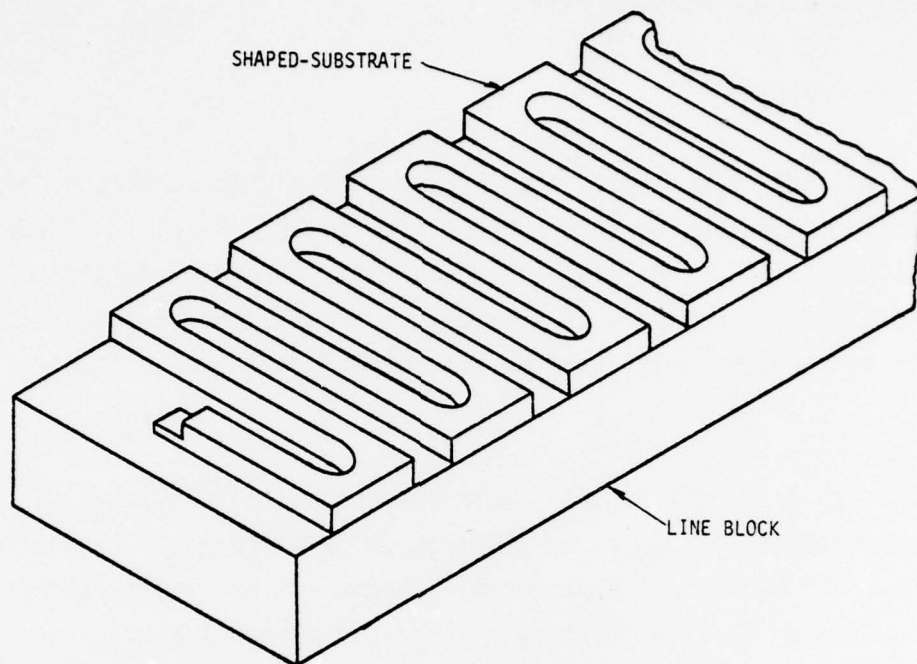
### 2.1 General Approach

The principal objective of the study of the shaped-substrate meander line was to verify the performance characteristics of an IBCFA which incorporates such a design concept. The test vehicle was a standard production CFA, type RW-619, modified as necessary to incorporate a simulated shaped-substrate meander line, together with gun modifications appropriate to the new line width.

It appears difficult if not impossible to fabricate a low-cost ceramic meander substrate suitable for an IBCFA by grinding or other conventional technology. ECOM personnel have recently begun to investigate the fabrication of such substrates by laser cutting. A meander-shaped substrate on a supporting block is shown in Figure 1; the ECOM designed laser-cut ladder-shaped substrate, with approximately equivalent electrical properties, is shown in Figure 2.

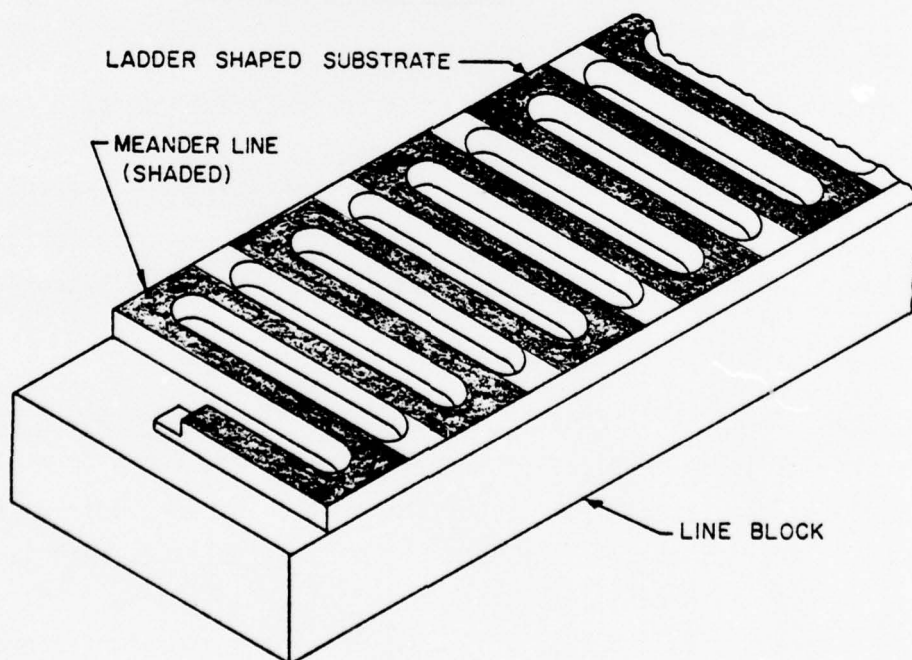
For comparison, the structure used in previous CFA designs is shown in Figure 3. Here the meander line is supported on individual ceramic insulators, and vanes between meander line segments are added to reduce dispersion of phase velocity as a function of frequency. The ECOM design is intended to reduce costs by replacing these individual bars with a one-piece substrate, and by achieving the required low dispersion without the vanes between segments.

For the purpose of this investigation, the shaped-substrate was simulated by an array of individual ceramics of suitable length and cross section, as shown in Figure 4. The electrical properties of the shaped-substrate are duplicated with ceramics easily fabricated by well established techniques. The matching of thermal expansions is not critical in this case. The individual ceramics are set in grooves, following present production techniques. This has the advantage of locating the position of the bars accurately. Its performance characteristics are identical to the shaped-substrate if the groove depth is adjusted so that the line-to-ground capacitance is the same.



156-022984

Figure 1. Shaped-Substrate on Line Support Block.



156-022984

Figure 2. Ladder-Shaped Substrate with Meander Line.

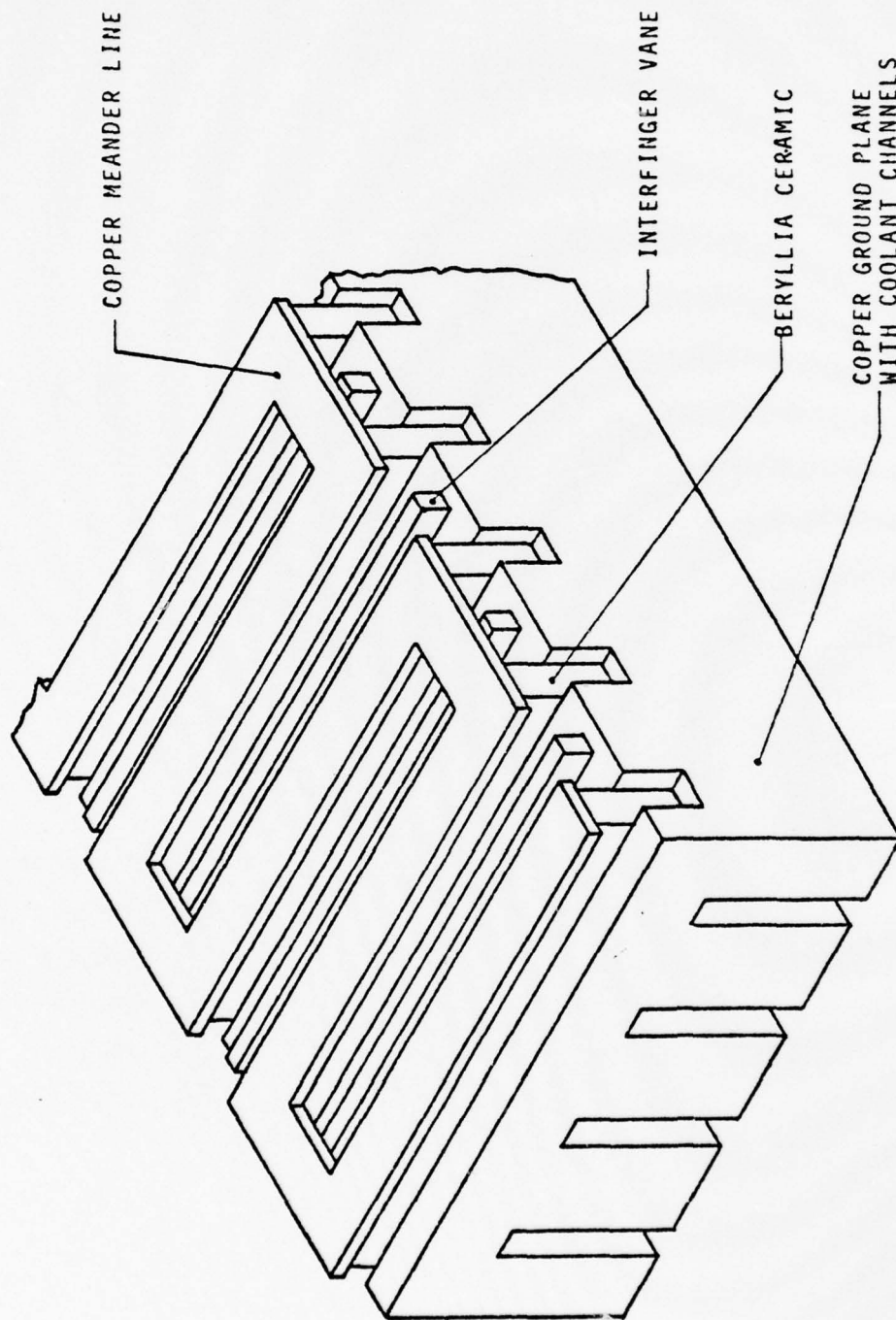


Figure 3. Meander Line (Vane Configuration Indicated).

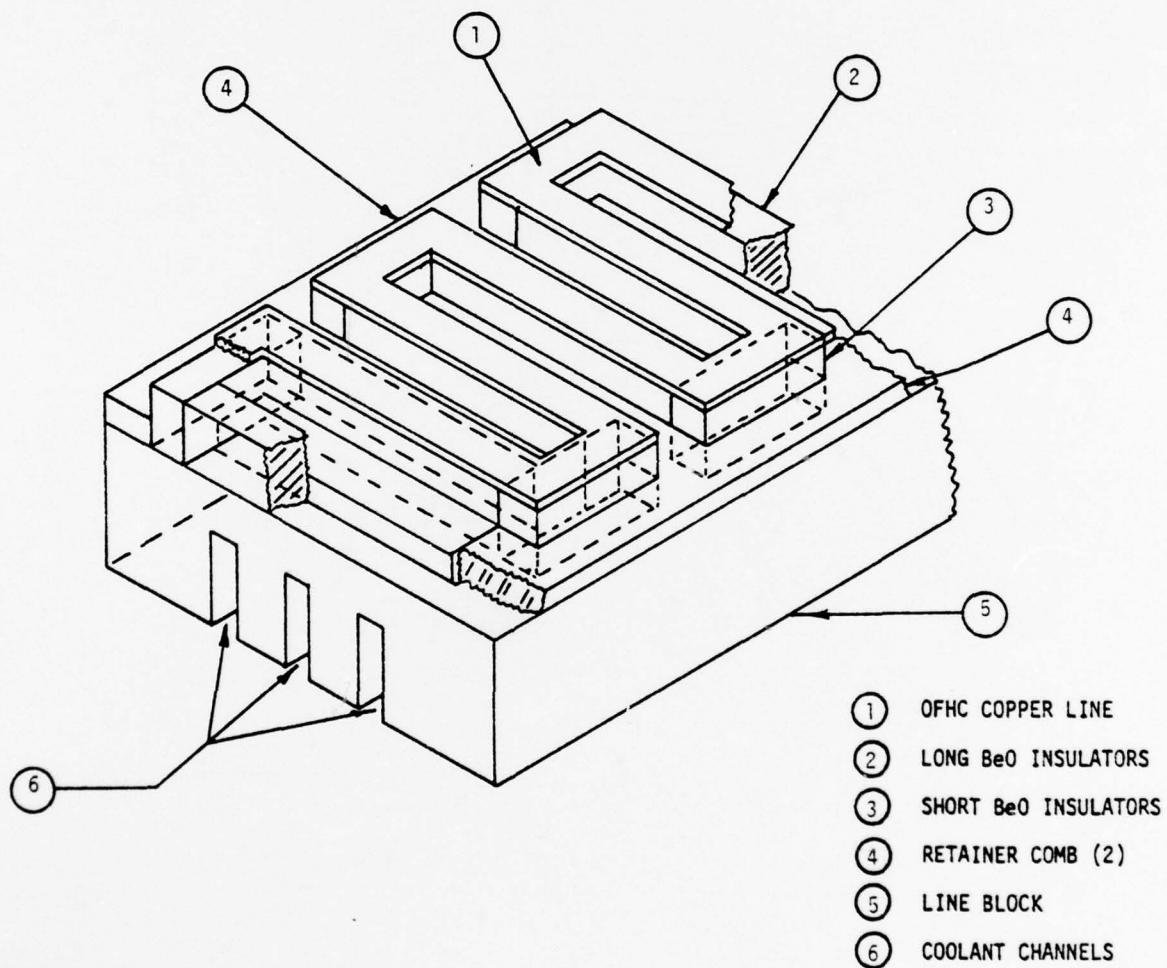


Figure 4. Shaped-Substrate Meander Line: Multiple Insulators in Grooves.

This approach is not of itself low cost. However, its performance demonstrates the electrical characteristics of an IBCFA with a shaped-substrate meander line.

## 2.2 Cold-test Models

The first undertaking was to explore experimentally the electrical properties of the shaped-substrate meander line: phase velocity and dispersion, characteristic impedance, and coupling impedance. For convenience in fabricating the initial experimental model, the dimensions were chosen to be twice those given in the Statement of Work (Technical Guidelines MW-104), which were based on previous studies by Bates and Hartley of ECOM. The substrate thickness was modified to take into account the grooves (0.010" deep) into which the insulators were set. The beryllia ceramic material was simulated by Stycast HiK 6 (Emerson & Cuming). The structure was like Figure 4, except liquid cooling was not required.

Measurements of the initial model indicated values of  $c/v$ , the delay ratio, lower than desired (see curve 1, Figure 5). Increasing the width led to a satisfactory range of delay ratios (curve 2, Figure 5), but an impedance of 60 ohms instead of the 50 ohms specified by ECOM. Reducing the insulator thickness gave an impedance of 50 ohms, and slightly greater delay ratio (curve 3, Figure 5). The last of these was used as the basis for the design of the operating tube, scaling in wavelength from an "operating band" shown in Figure 5 so that the phase shift of  $\pi/2$  radians per bar would occur at approximately 3.5 GHz. The pitch was scaled further to give a value of delay ratio of 17.2 at midband, the same as the RW-619. The actual dimensions in each of these models are summarized in Table 1.

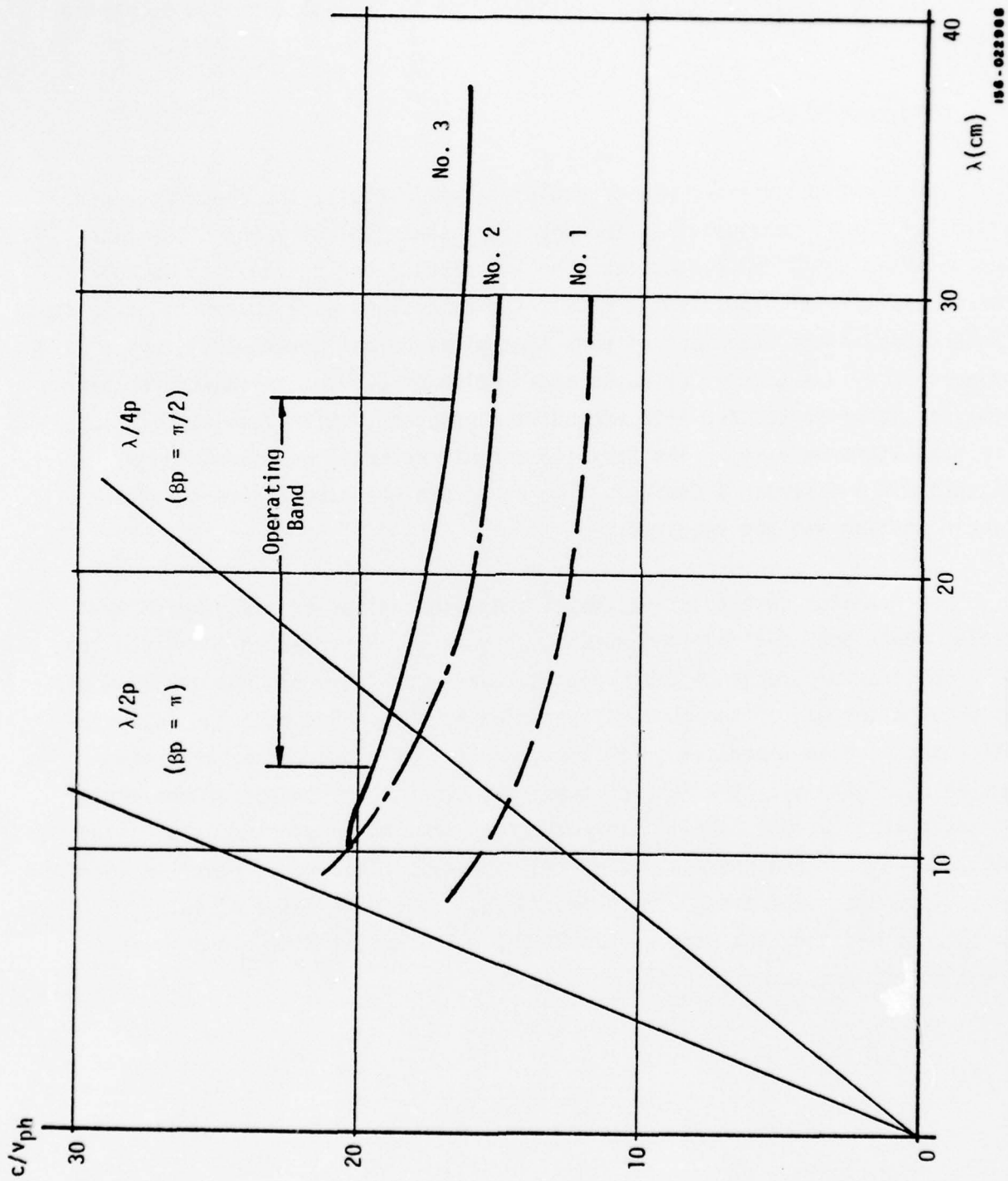


Figure 5. Delay Ratio: Cold-Test Meander Lines for Low Cost CFA.

Table 1. Summary of Cold Test Models.

	Technical Guidelines (S-Band line)	Model No. 1 (L-Band Cold test lines)	Model No. 2	Model No. 3
Height (in.)	0.420	0.840	1.008	1.008
Pitch (in.)	0.040	0.080	0.080	0.080
Substrate Thickness (in.)	0.014	0.035*	0.035*	0.030*
Metal-to-Space Ratio	1:1	1:1	1:1	1:1
Characteristic Impedance (ohms)	50	--	60	50

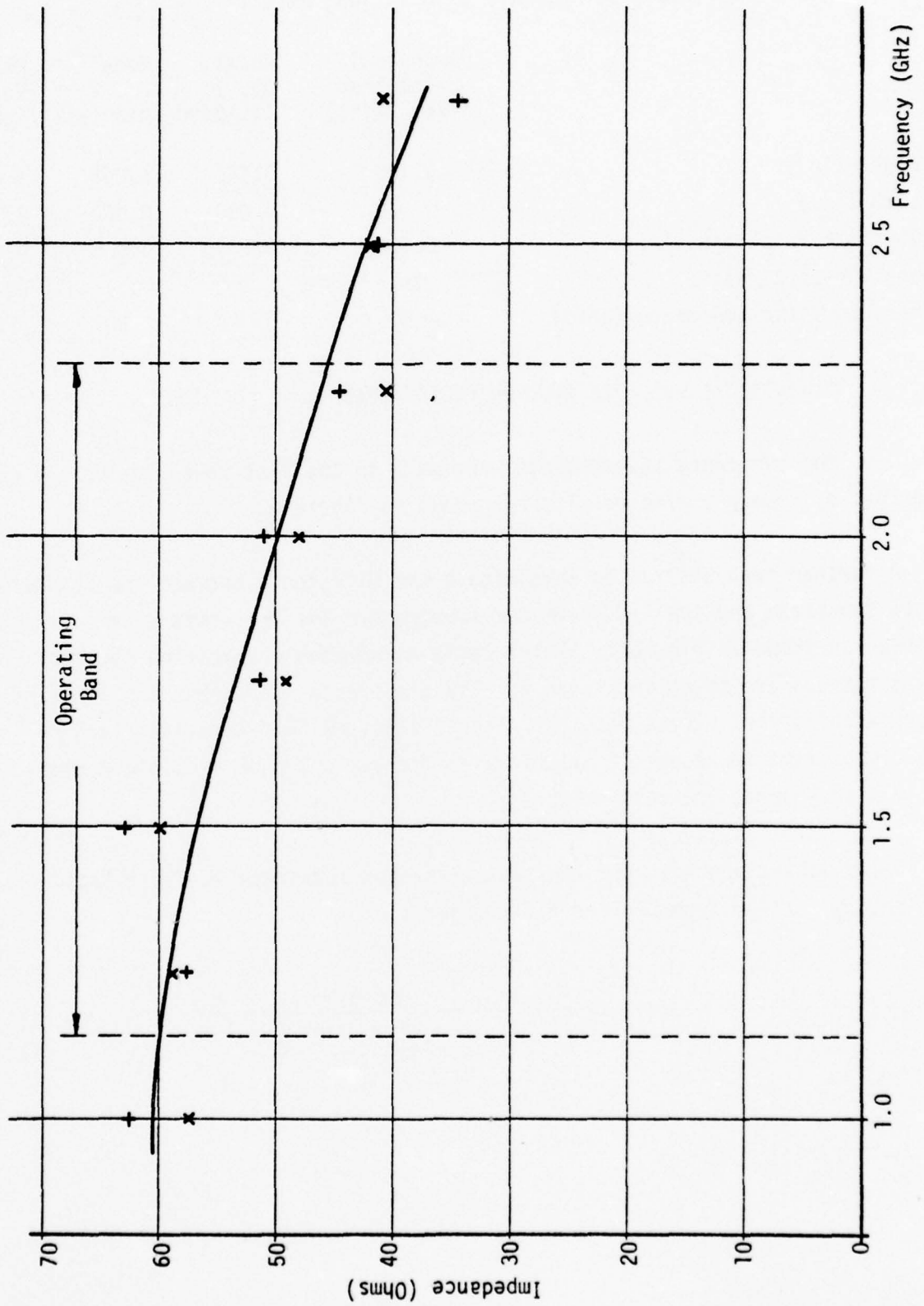
\*Insulators set into grooves 0.010" deep

Coupling impedance measurements were made on the last model, using the method described by Arnaud<sup>1</sup>. The results are shown in Figure 6.

A further test was run to investigate the difference between the meander-shaped substrate and the ladder-shaped substrate. The cold-test model was modified as shown in Figure 7. Delay ratio measurements comparing the two configurations are shown in Figure 8. The difference approaches the limit of experimental error. These results indicate that the ECOM-developed ladder-shaped substrate represents a practical electrical approach to achieve ultimately a one-piece, low-cost substrate.

Delay line dispersion for the meander shaped substrate was correlated with theory derived from Leblond and Mourier<sup>2</sup>:

$$\cos kw = \frac{\cos \phi}{1 + \frac{2\gamma_1}{\gamma_0} \sin^2 \phi} \quad (1)$$



156-022989

Figure 6. Coupling Impedance: Cold-Test Meander Line For Low Cost CFA.

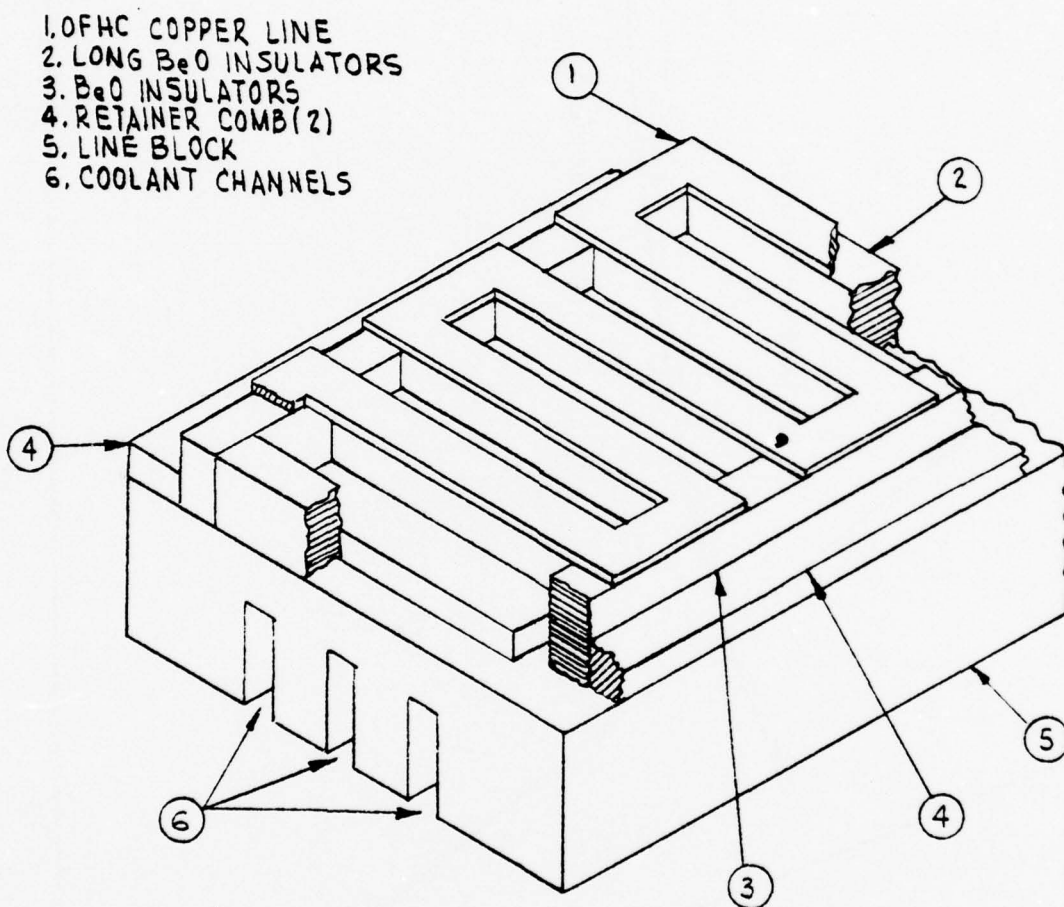


Figure 7. Simulated Ladder-Substrate Meander Line: Multiple Insulators In Grooves.

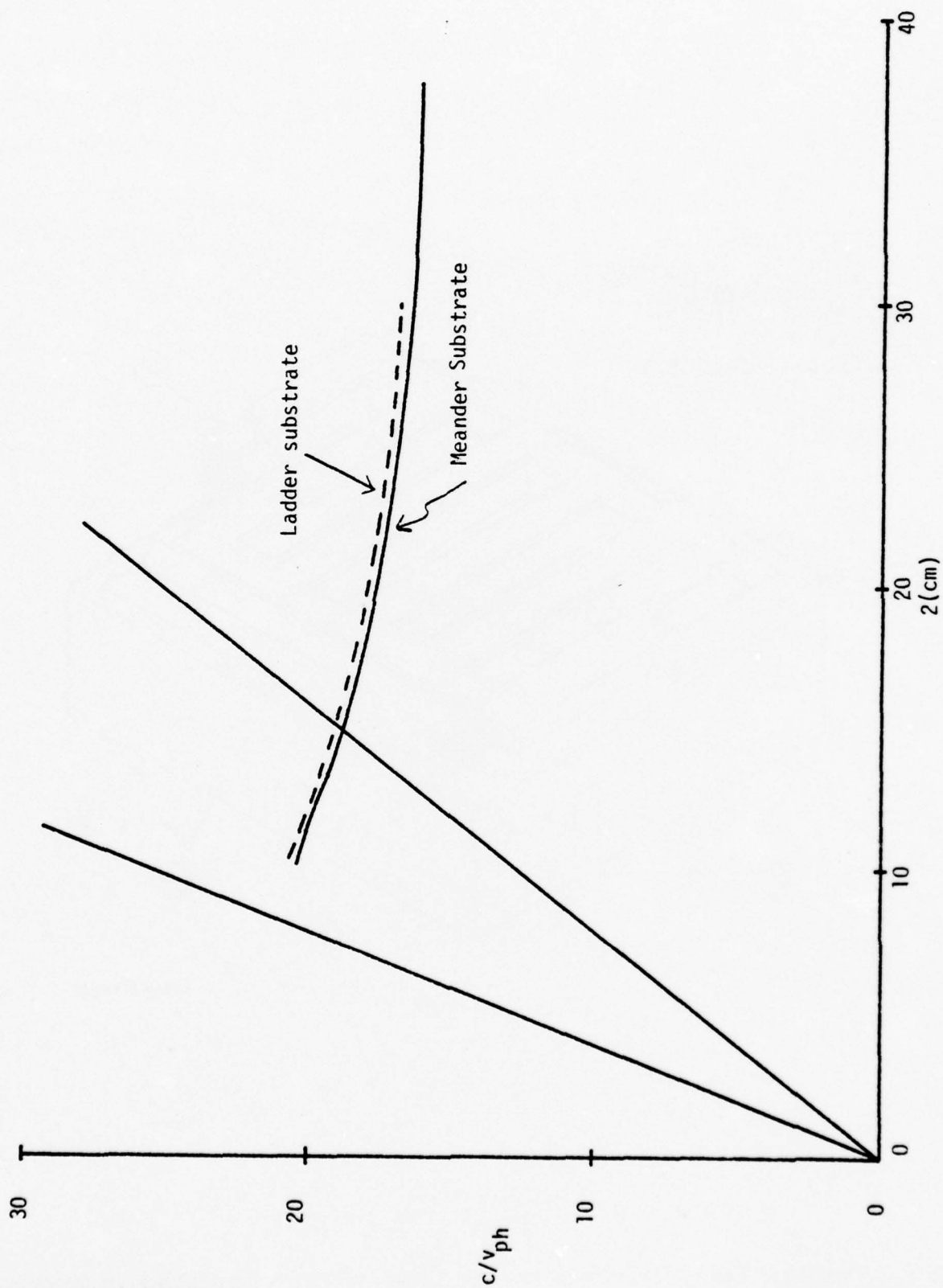


Figure 8. Delay Ratio of Meander Line With Ladder Substrate Compared With Meander Substrate.

156-022990

In the above:

- $\kappa$  = Propagation factor of a wave along the length of a delay line bar
- $w$  = Length of each bar (width of the line)
- $\phi$  = Phase between one bar and the next =  $\beta p$
- $\gamma_1$  = Capacity per unit length between two adjacent bars
- $\gamma_0$  = Capacity per unit length from one bar to ground (base plate)

Calculated results show an excellent fit for  $\gamma_0/\gamma_1 = 7.5$  and  $\kappa/\kappa_0 = 1.47$ , where  $\kappa_0$  is the free space propagation factor given by  $\omega/c$ .

The delay line design characteristics derived from the cold test measurements are summarized in Table 2.

### 2.3 Electrical Design of Operating CFA

The electrical design of the CFA with shaped-substrate meander line was made to be like the production type RW-619 in all respects where appropriate. For example, since the frequency range and phase velocities were approximately the same, the sole-to-line spacings were the same. Since the width of the line used here was greater than that of the RW-619, the sole, gun, collector and pole-piece gap were widened accordingly.

Some approximate calculations of small-signal gain using the work of Gould<sup>3</sup>, and large signal characteristics using the work of Sobotka<sup>4</sup>, were carried out. The rate of gain over the frequency band was calculated to be at least as great as the RW-619, so that no change of over-all line length (about three inches) appeared necessary.

Since a revision of the gun was required, a recently developed improvement in grid design, not yet introduced in the RW-619, was used in this CFA. The grid openings were extended around the front edge of the grid box, as described by Dohler<sup>5</sup> (see Figure 9).

Table 2. Low Cost CFA With Simulated Shaped Substrate: Line Specifications.

	<u>ECOM Statement of Work</u>	<u>CFA Design</u>
Characteristic Impedance (ohms)	50	50
Circuit Height (inches)	0.42	0.576
Circuit Pitch (inches)	0.040	0.048
Circuit Length (inches)	3.0	3.0
Substrate Thickness (inches)	0.014	0.012*
Frequency for 90° Phase Shift (GHz)	3.0-3.5	3.5
Number of Circuit Elements	75	62
Circuit Metal-To-Space Ratio	1:1	1:1
Copper Line Thickness (inches)	---	0.015

\*Projection above line block: Groove depth = 0.0175".

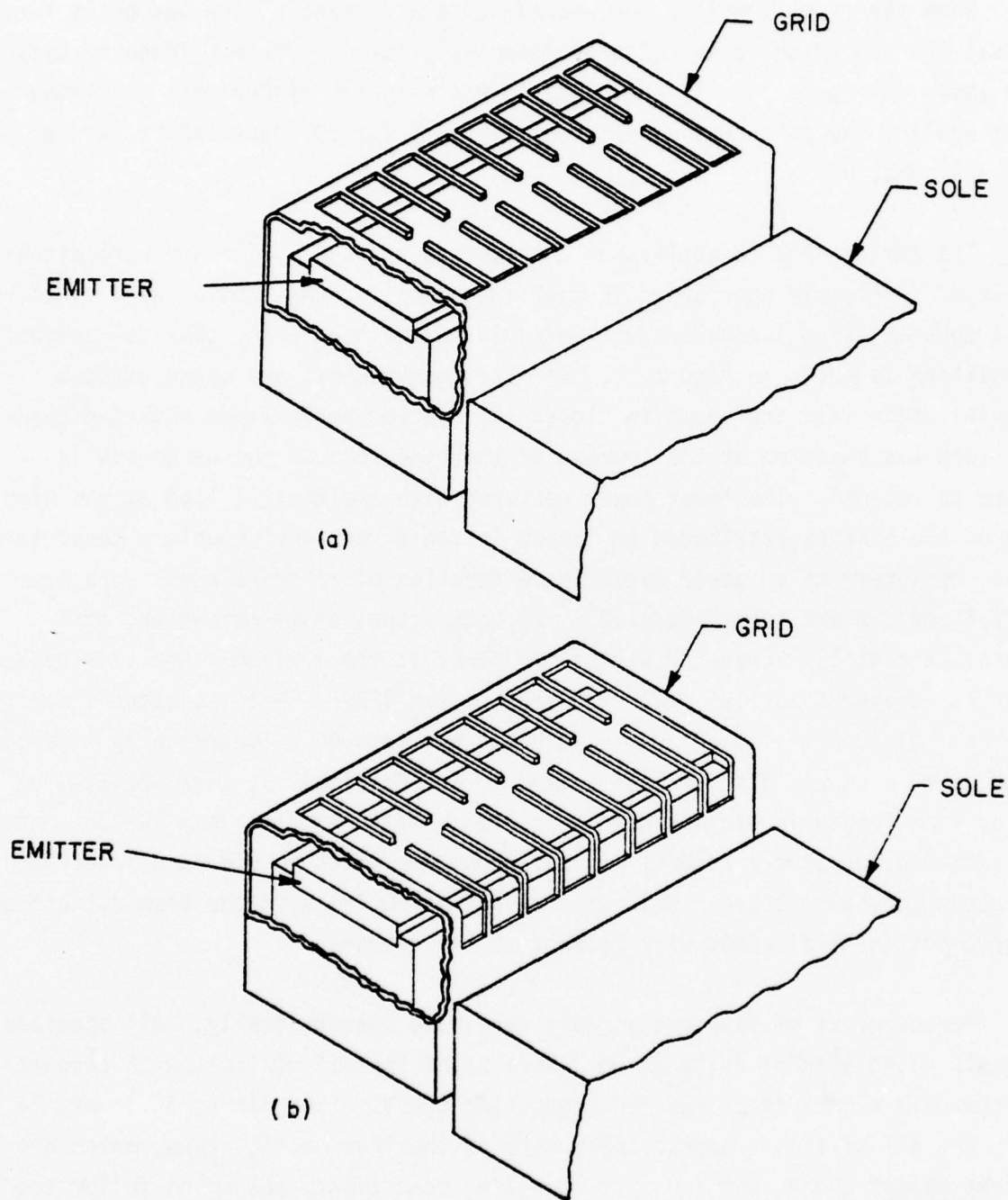
Measured Characteristics

Delay Ratio (c/v)

	<u>Frequency (GHz)</u>		
	<u>2.0</u>	<u>3.0</u>	<u>4.0</u>
Shaped-Substrate Design	16.0	17.2	18.4
Production CFA	16.2	17.2	18.1

Coupling Impedance At Level Of Line (ohms)

	<u>Frequency (GHz)</u>		
	<u>2.0</u>	<u>3.0</u>	<u>4.0</u>
Shaped-Substrate Design	59	52	45
Production CFA	52	50	47



156-022991

Figure 9. (a) Initial Grid Design.  
(b) Improved Grid Design With Openings Extended Over Edge Toward Interaction Space.

## 2.4 Operating Characteristics

When the first model of the shaped-substrate meander line was built for actual CFA operation, cold tests of phase velocity were made. These results are shown in Figure 10. The delay ratio was slightly higher than predicted from scaling the cold-test model; the frequency for  $90^\circ$  phase shift per bar was 3.33 GHz.

The performance objectives of 3 kW output and 35% efficiency were either achieved or closely approached in the first model. Power output as a function of frequency using a double-ridge waveguide water load and a coax-to-waveguide transition is shown in Figure 11. Similar measurements are shown using a coaxial water load are shown in Figure 12. Better performance with the coaxial load was expected at the low end of the band because the waveguide is close to cut-off. The lower power measured with the coaxial load at the high end of the band is attributed to losses in the directional coupler, connectors, etc. Measurements of power output as a function of rf drive power were made at 2.8 and 3.0 GHz (see Figure 13). In both cases, power output and efficiency were still increasing with drive power at the maximum power attainable with the driver tube (120 W at the input to the CFA). This indicates that the over-all gain of the tube can be increased by means of a longer delay line to produce more power, gain, and efficiency. An additional 10 bars (0.480") of delay line length is estimated to be needed. Maximum efficiency was 36%, not including drive power. Useful instantaneous bandwidth in mid-band appears to be about one-half octave. Grid control was effective with the beam cut off at a grid potential of -640V with respect to the cathode.

Measurements of spurious signals were made systematically. All spurious signals found with rf drive at 30 W were below the -15 dB limit with respect to the main signal specified for production tubes. (See Figure 14.) Nearly all, and all of the strongest ones, were of the "parametric" type, which are absent except under non-linear rf operating conditions, and which follow the pattern:

$$f_s = mf_0 - nf_d$$

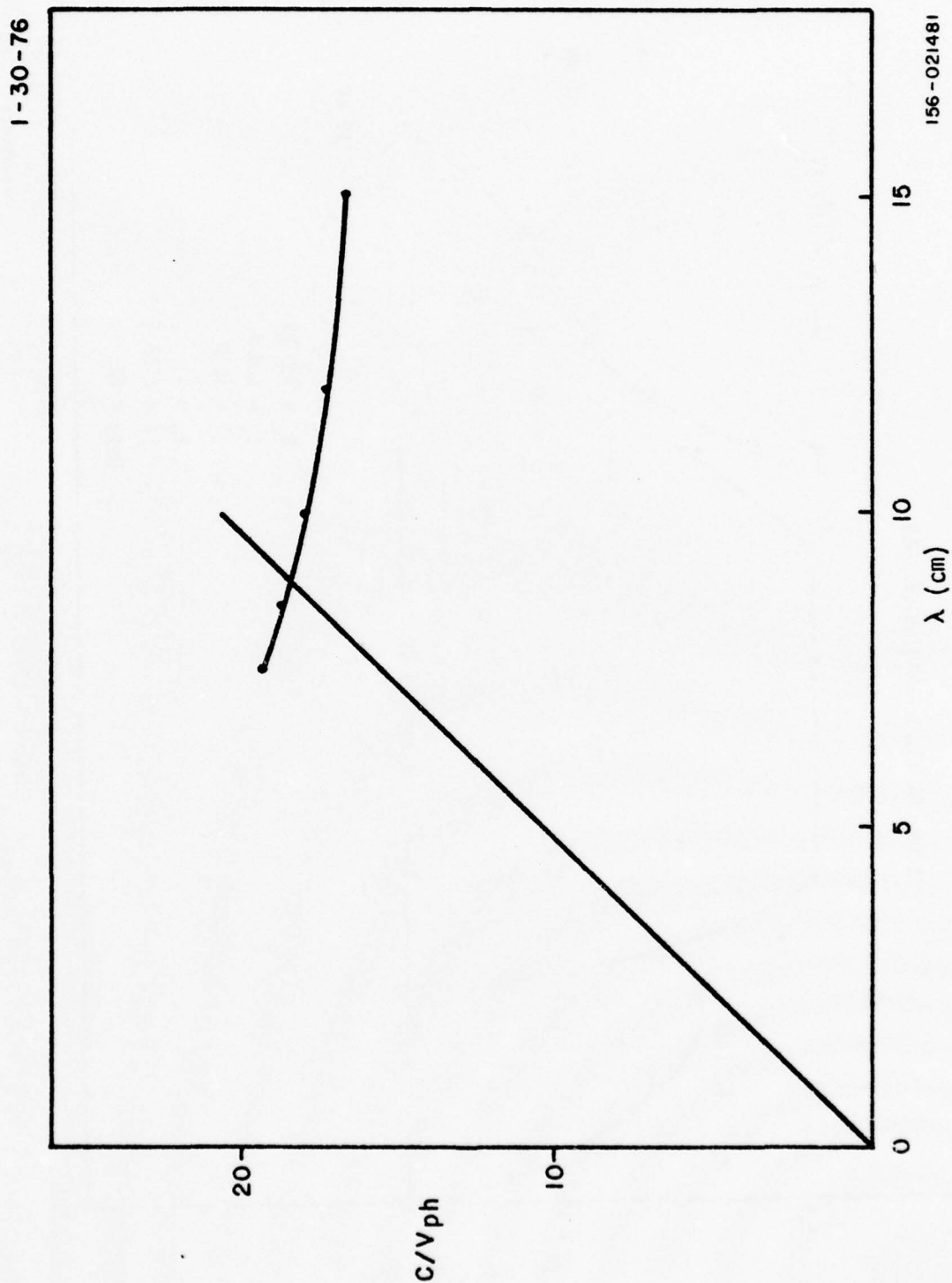


Figure 10. Delay Ratio of First CFA Model.

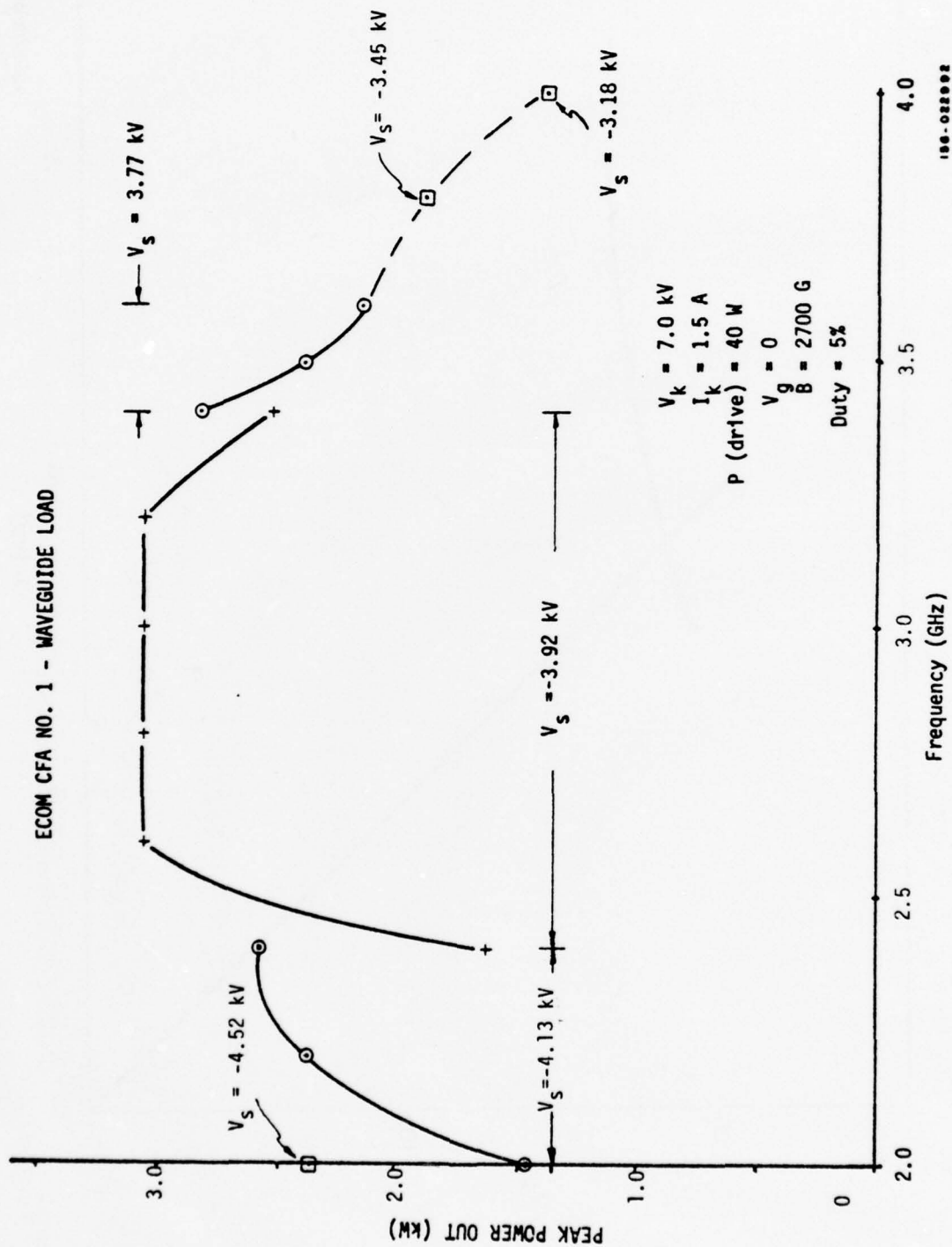


Figure 11. Power Output of IBCFA With Waveguide Load.

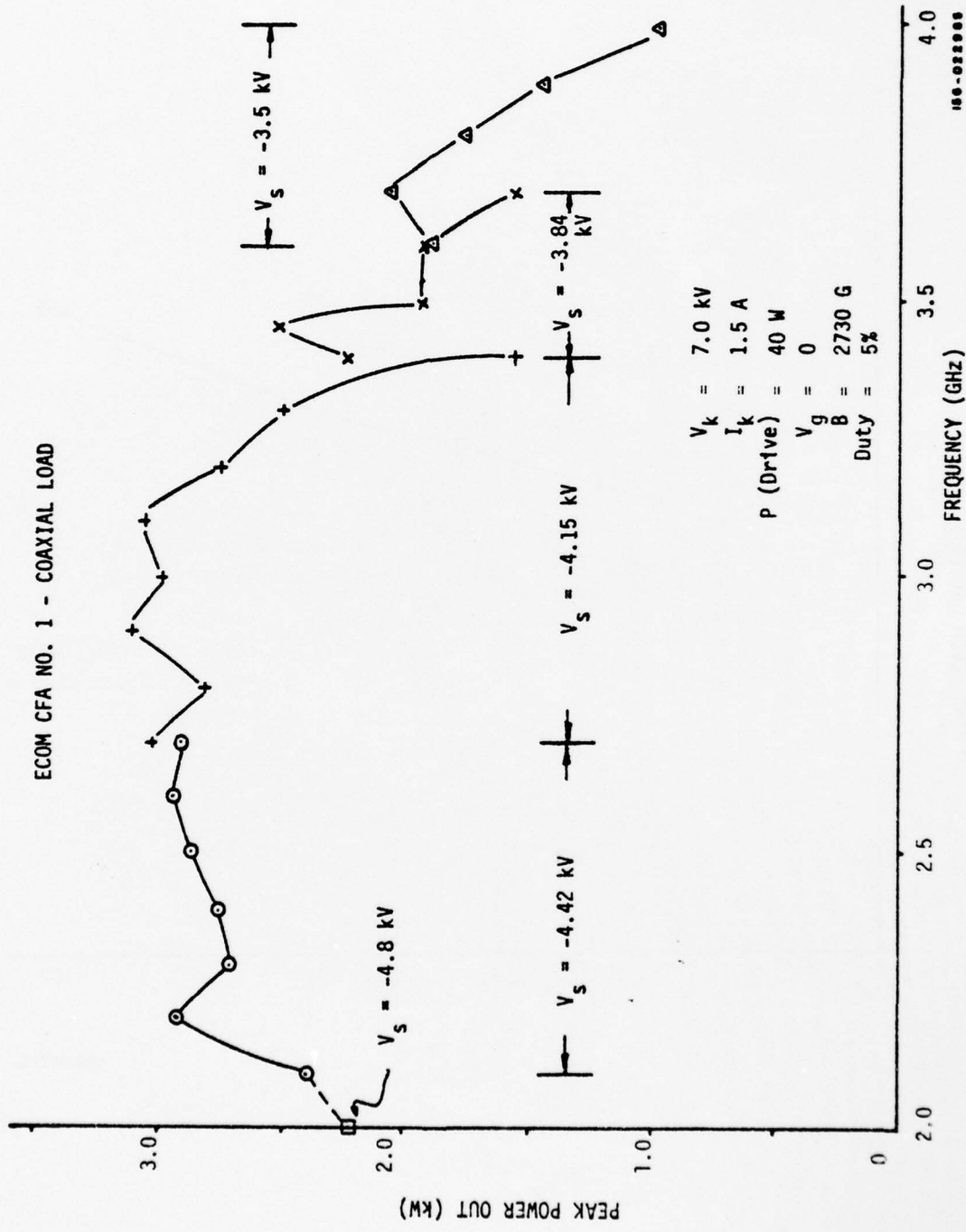
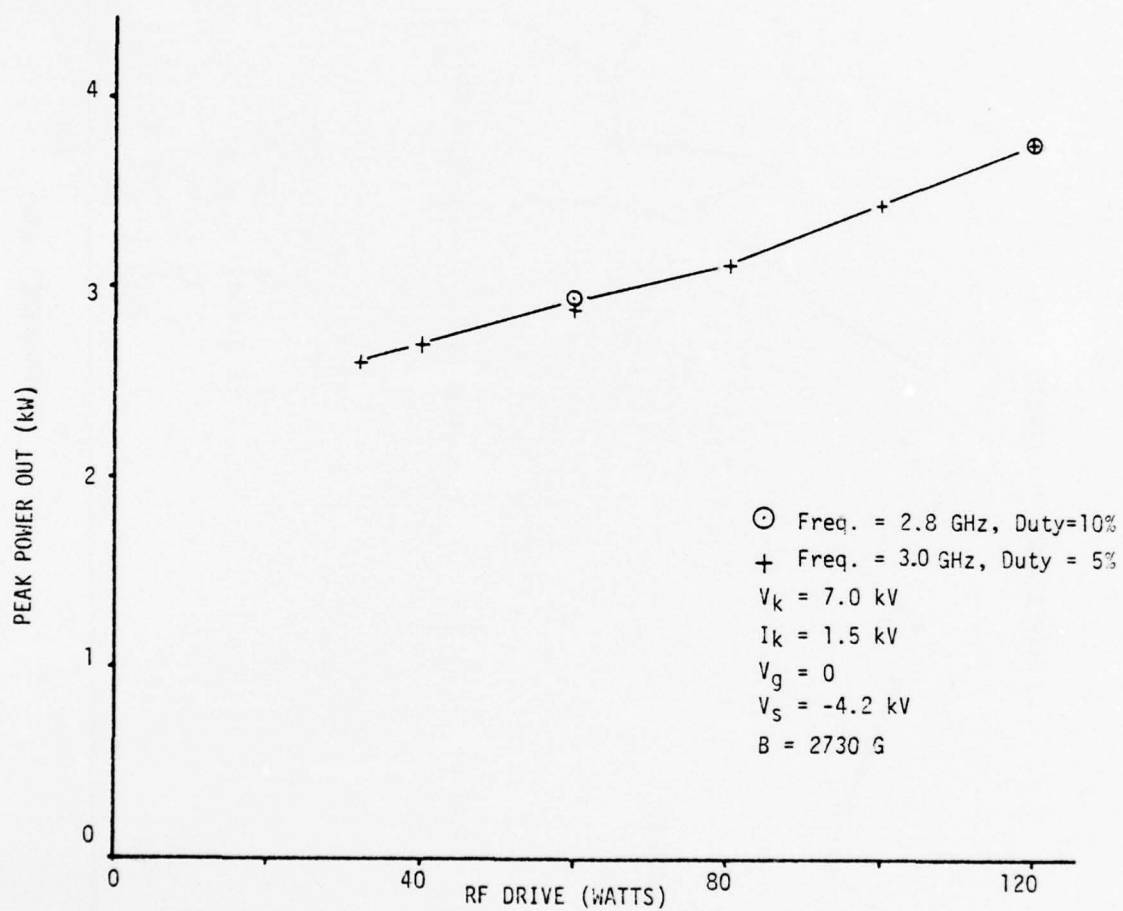


Figure 12. Power Output of IBCFA With Coaxial Load.



156-022993

Figure 13. Power Output of IBCFA With Coaxial Load as a Function of RF Drive Power.

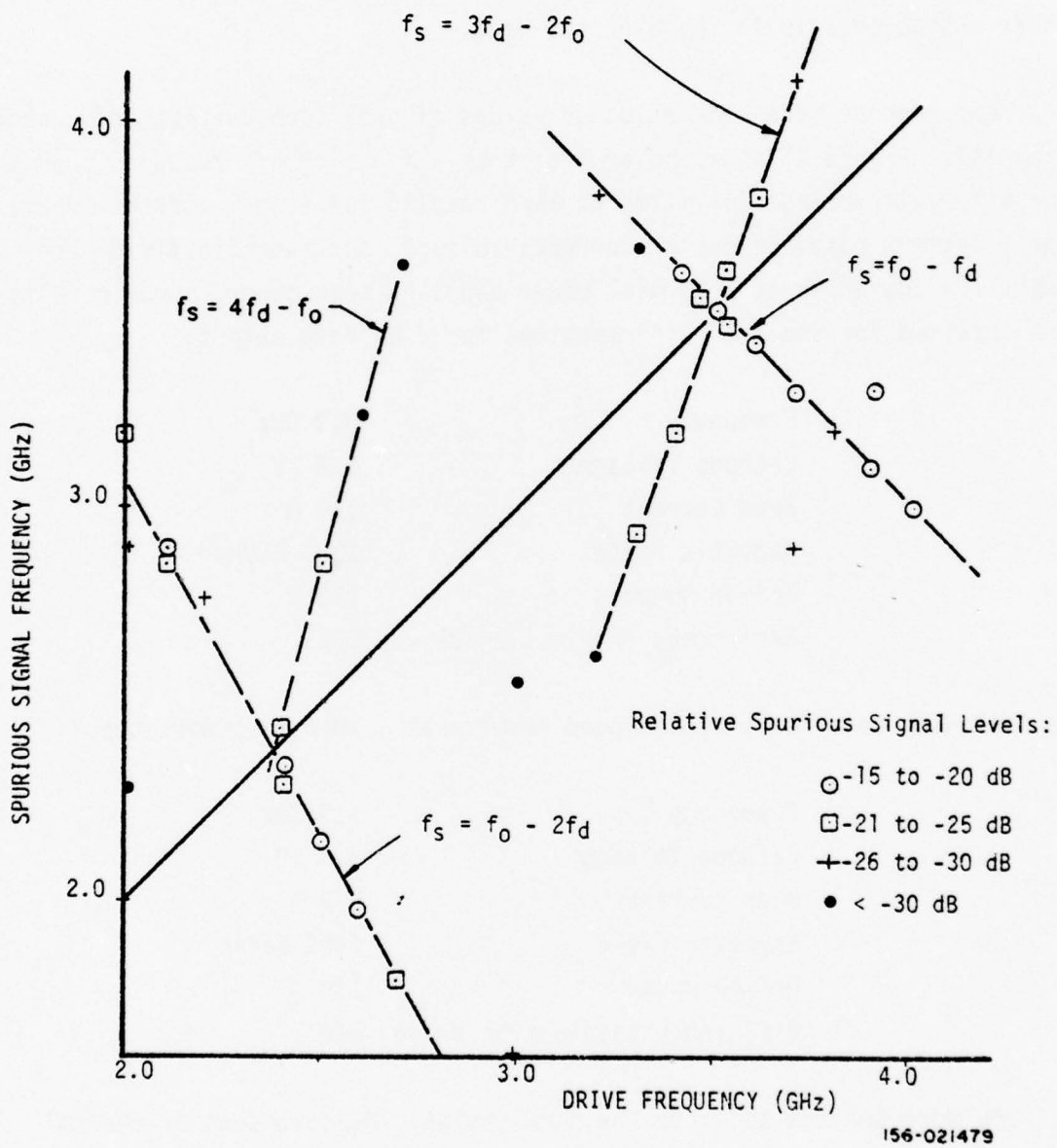


Figure 14. Spurious Signals in IBCFA. (ECOM CFA No. 1)

where  $m$  and  $n$  are integers. The strongest pattern corresponded to  $m = 1$  and  $n = 1$ . Others were found for  $m = 1, n = 2$ , for  $m = -2, n = 3$ , and for  $m = -1, n = 4$ . In all of these cases,  $f_0 = 7.02$  GHz, which corresponds to the upper edge of the first stop band. No oscillations are found at this frequency except in the presence of an rf drive signal strong enough to produce a non-linear characteristic in the electron beam.

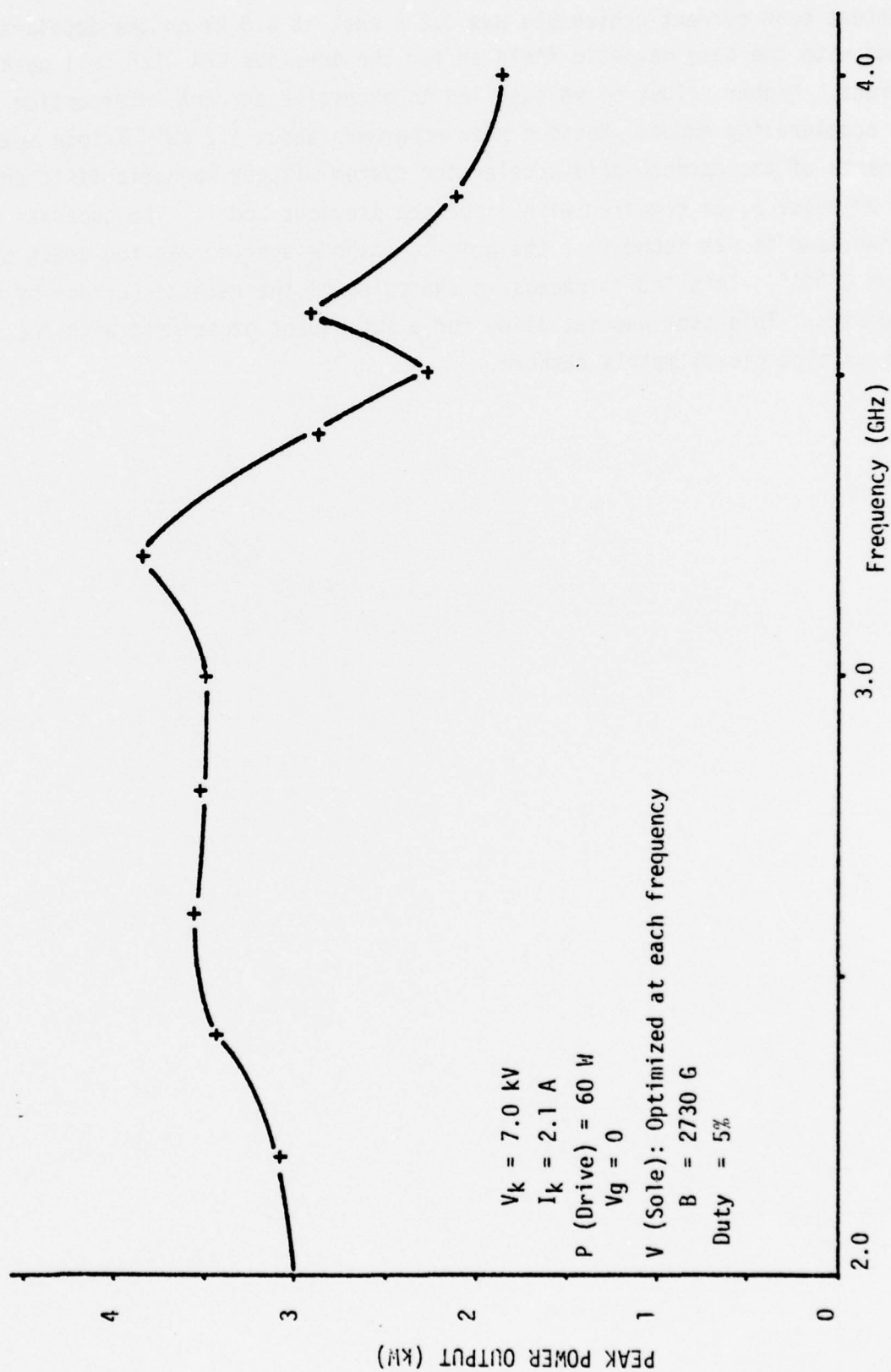
Measurements were made at other values of peak beam current and cathode potential. Figure 15 shows power output as a function of frequency over the band with sole voltage optimized at each reading for a beam current of 2.1 A peak. Optimum combinations of current, voltage, and magnetic field were sought for operation at 2 kW peak power and 1 kW peak power. Good results were obtained for the following settings for 2 kW peak output:

Frequency	3.0 GHz
Cathode Voltage	5.8 kV
Beam Current	1.0 A
Magnetic Field	2200 Gauss
Driver Power	120 W
Efficiency (neglecting drive)	34%

The following settings produced good results at 1 kW peak power output:

Frequency	3.0 GHz
Cathode Voltage	5.0 kV
Beam Current	0.7 A
Magnetic Field	2100 Gauss
Driver Power	120 W
Efficiency (neglecting drive)	28%

One more CFA was built to the same design. Measurements of thermal conductivity from the meander line to the support block indicated much better bonding than the first tube. This line should have been capable of full specification average power with a comfortable margin. When tested, this model required excessive accelerating anode voltage for operation. The



136-022994

Figure 15. Power Output of IBCFA with Increased Beam Current. (ECOM CFA No.1)

greatest beam current achievable was 1.2 A peak at 4.8 kV on the accelerating anode with the same magnetic field as for the previous CFA with full peak current. Higher values of voltage led to excessive current interception by the accelerating anode. Maximum peak power was about 1.2 kW. Triode measurements of the cathode-grid-accelerator system without magnetic field showed a  $\mu$  of about 8, as compared with 4 for the previous model. The tube was opened, and it was found that the grid-to-cathode spacing was too great by about 0.004". This led to excessive shadowing of the cathode surface by the grid bars. This tube was set aside for a subsequent experiment with the Medicus type nickel matrix cathode.

### 3. FLAT SUBSTRATE MEANDER LINE

#### 3.1 General Approach

A still lower cost method of meander line construction is a flat continuous substrate instead of the shaped substrate. Possible disadvantages of the flat substrate are:

- (1) Greater dispersion and therefore reduced bandwidth;
- (2) Area between bars subject to metallization by evaporation or sputtering, leading to deterioration of performance.

The performance objectives were the same as before.

To make use of parts common to production CFA's while obtaining an adequate evaluation of the performance of a CFA with a flat-substrate meander line, the flat substrate was simulated by an arrangement of individual bars. The manner of simulation is comparable with that used to simulate the shaped substrate; the only difference is adding additional dielectric material between the individual line support ceramics, as in Figure 16.

#### 3.2 Cold-Test Model

To arrive at the actual dimensions to be used on the line, the same large-scale meander structure used previously (see Section 2.2) was rebuilt with a flat substrate instead of the simulated shaped substrate. As before, the substrate was made of Stycast HIK6. The thickness was adjusted experimentally to produce a characteristic impedance of 50 ohms. Phase velocity measurements were then made from which the values of  $\kappa/\kappa_0$  (the dielectric loading) and  $\gamma_0/\gamma_1$  (the ratio of bar-to-ground capacitance to bar-to-bar capacitance) could be determined. (See Equation (1), Section 2.2). Previous experience, including the work described earlier in this report, indicates that if these quantities are known, the width of the line (length of each bar) can be adjusted for the correct delay ratio. The requirement is that all

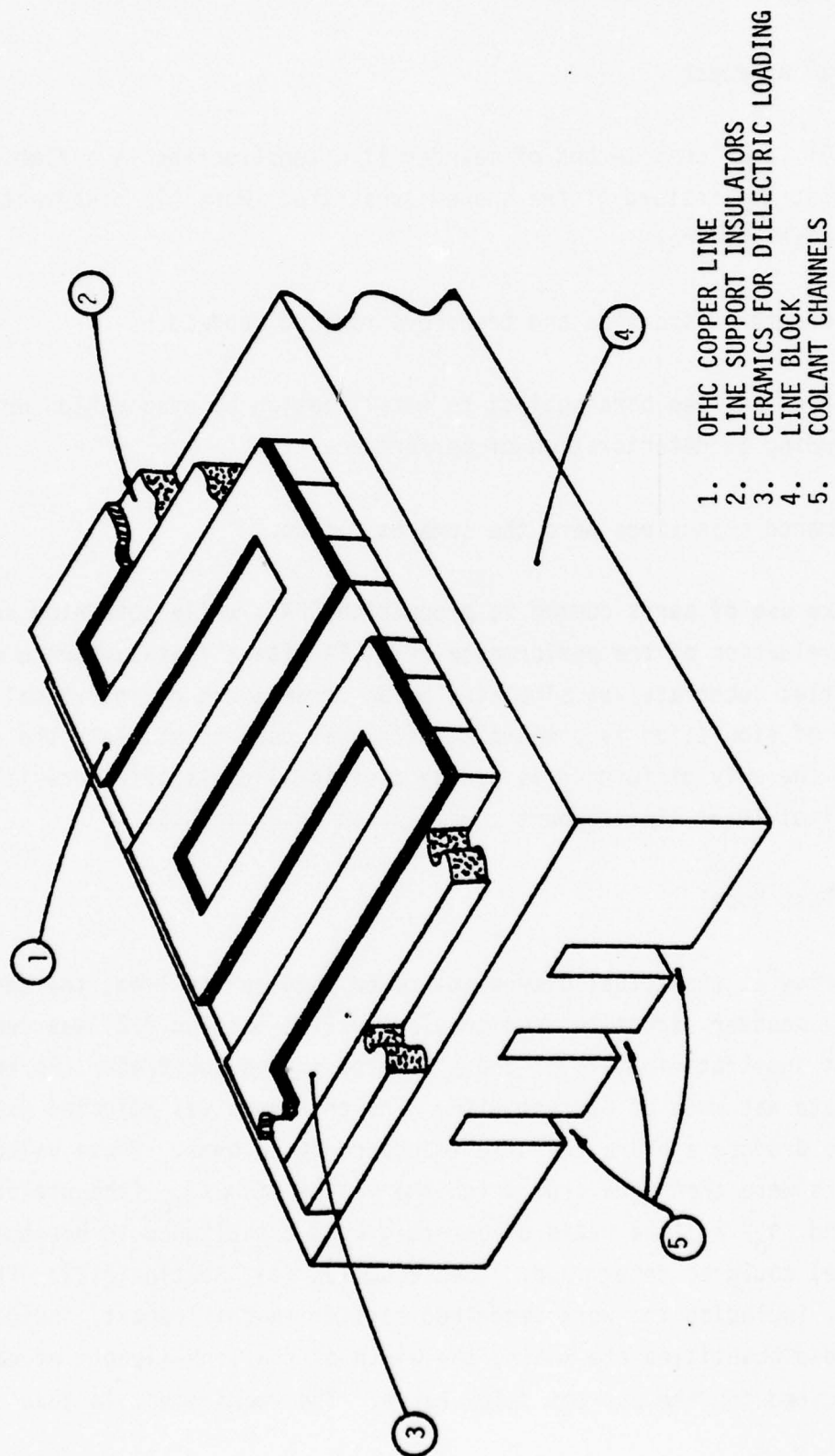


Figure 16. Meander Line With Increased Dielectric Loading.

dimensions transverse with respect to the length of the bar be scaled faithfully. The values found from the cold-test model were:  $\kappa/\kappa_0 = 1.84$ ,  $\gamma_0/\gamma_1 = 11$ . The values of  $\gamma_0/\gamma_1$  found from cold test correspond to quite low dispersion.

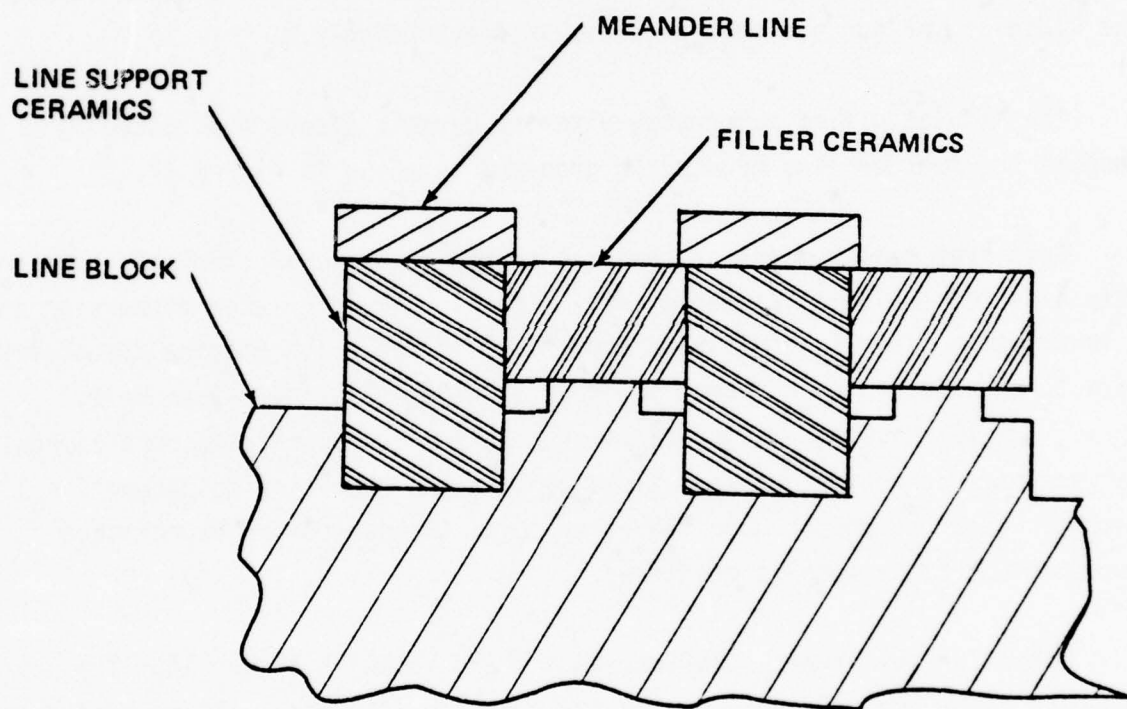
### 3.3 Operating CFA with Simulated Flat Substrate

The cold test results indicated much higher dielectric loading (i.e.,  $\kappa/\kappa_0$ ) in the flat substrate configuration than in the shaped, as expected. Consequently the line width was substantially less: 0.480" instead of 0.576". The width of the gun and sole were adjusted accordingly.

The simulated flat substrate, with the ceramic pieces that actually support the meander line mounted in grooves, is shown in Figure 17.

Cold test measurements of the line showed higher characteristic impedance than expected (60 ohms instead of 50). It also showed greater dispersion and a lower delay ratio. Results are summarized in Table 3. Fitting the observed data to the dispersion characteristic of Equation (1), the values were:  $\kappa/\kappa_0 = 1.77$ ,  $\gamma_0/\gamma_1 = 6.1$ . In simulating the flat substrate, the approximations made to achieve an equivalent capacitance from line to ground ( $\gamma_0$ ) were not accurate enough. On the other hand, the bar-to-bar capacitance remained about the same as predicted.

Operating performance characteristics are shown in Figure 18. The magnetic field and voltage were set for optimum efficiency. Power output and efficiency were below what was expected from data on coupling impedance and attenuation. The sub-standard performance is attributed at least in part to the lower delay ratio than that for which the beam injection and interaction space were designed. There is an instantaneous bandwidth of 2.4 to 3.4 GHz where the optimum sole voltage was 3.0 kV, except for sole voltage adjustments made to improve power holes at 2.7 and 3.3 GHz. This range is better than expected. Measurements above 3.6 GHz are not included in Figure 18 because high levels of spurious signals made these values meaningless. The onset of strong spurious signals as frequency was raised above 3.6 GHz was quite abrupt.



156-022982

Figure 17. Cross Section of Simulated Flat-Substrate Meander Line.

Table 3. Low Cost CFA With Simulated Flat Substrate Line: Specifications.

	<u>Statement of Work</u>	<u>CFA Design</u>
Characteristic Impedance (ohms)	50	60
Circuit Height (inches)	0.42	0.480
Circuit Pitch (inches)	0.040	0.048
Circuit Length (inches)	3.0	3.0
Substrate Thickness (inches)	0.014	0.021*
Frequency for 90° Phase Shift (GHz)	3.0-3.5	3.5
Number of Circuit Elements	75	62
Circuit Metal-To-Space Ratio	1:1	1:1

\*Projection above line block: Groove depth = 0.0165".

Measured Characteristics

Delay Ratio (c/v)

	<u>Frequency (GHz)</u>		
	<u>2.0</u>	<u>3.0</u>	<u>4.0</u>
Flat Substrate Design	14.3	15.6	17.4
Production CFA	16.2	17.2	18.1

Coupling Impedance At Level Of Line (ohms)

	<u>Frequency (GHz)</u>		
	<u>2.0</u>	<u>3.0</u>	<u>4.0</u>
Flat Substrate Design	85	77	57
Production CFA	52	50	47

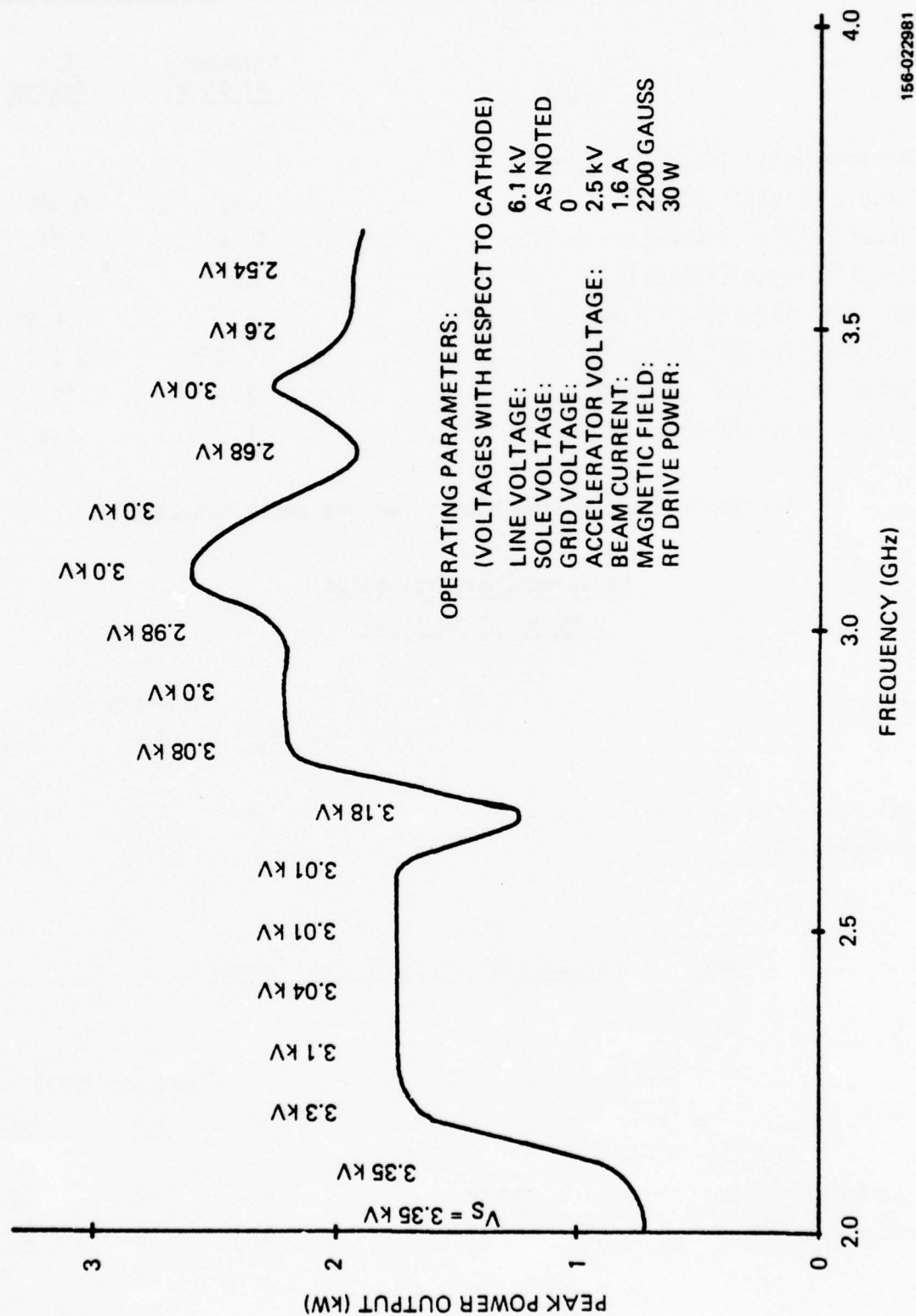
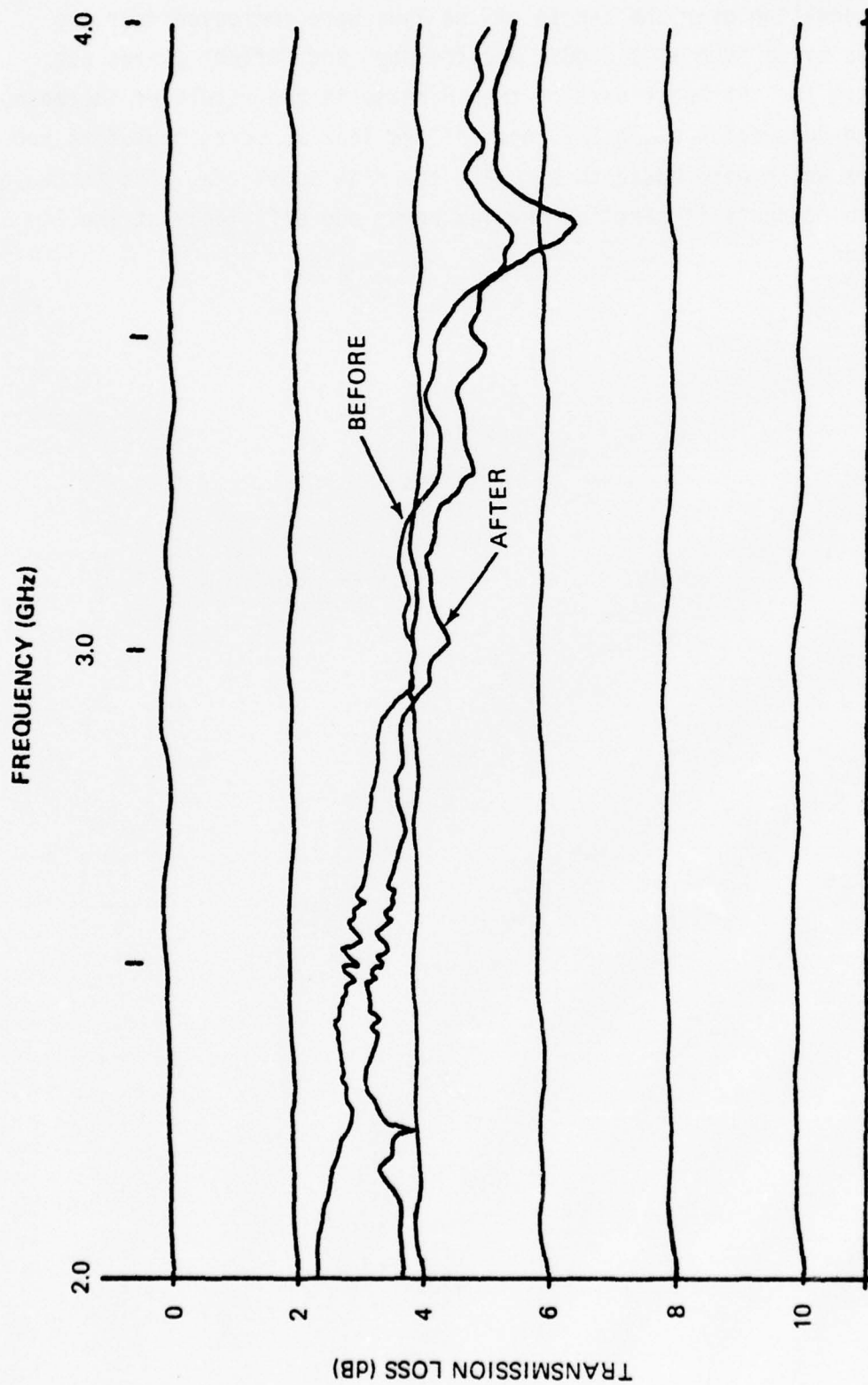


Figure 18. Power Output of Flat-Substrate IBCFA.

After operation, the meander line attenuation was re-measured. The values of attenuation over the length of the line were increased over the initial values by as much as 1.5 dB. The "before" and "after" curves are shown in Figure 19. At least part of the increase is the result of increased line-to-ground conduction along the edges of the line support insulators and the insulators which were added to simulate the flat substrate. The increase in attenuation accounts in part for the low power and efficiency at the low end of the band.



156-022980

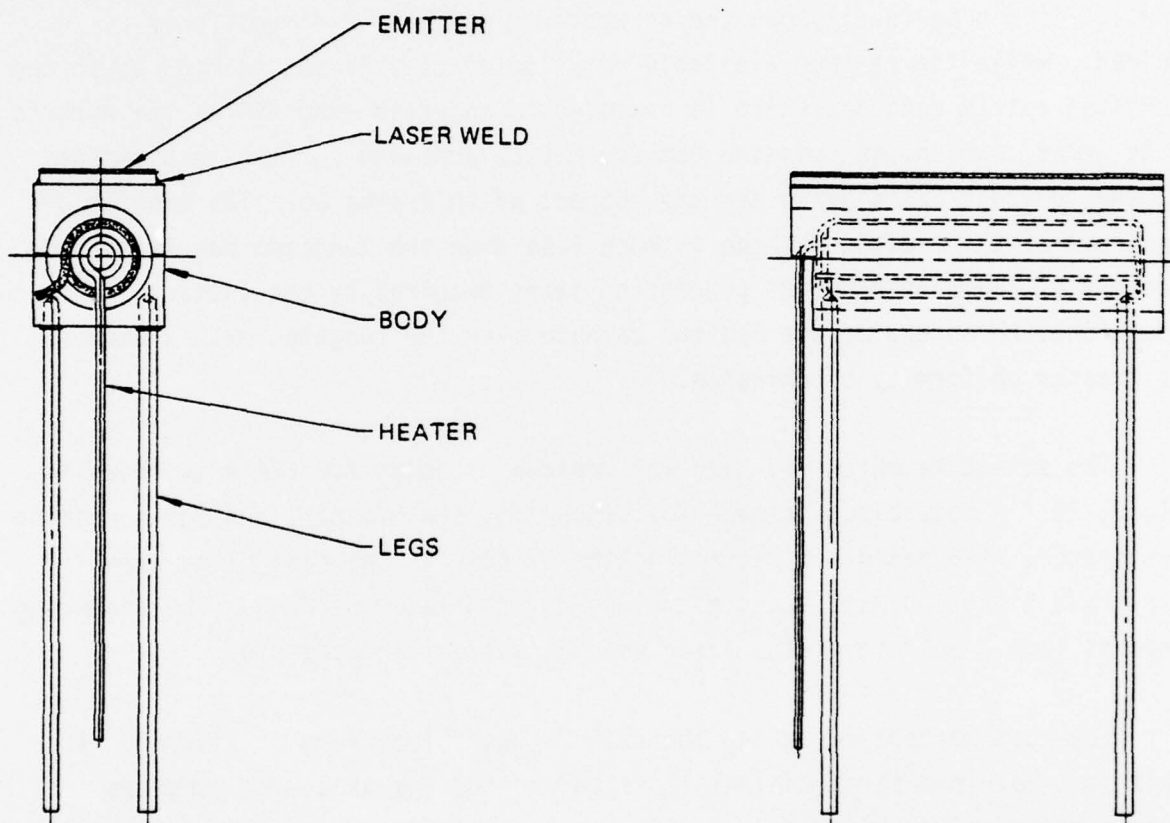
Figure 19. Transmission Loss In Simulated Flat-Substrate CFA Before and After Operation.

#### 4. MEDICUS NICKEL MATRIX CATHODE

The Medicus nickel matrix cathode represents an important advance over previous nickel matrix cathodes in its combination of high performance and potential for low cost. A mixture of nickel powder and alkaline earth carbonates is sintered on a nickel base, then rolled into a thin sheet in several steps with annealing between steps. The resulting sheet may be cut into appropriate sizes, or shaped when necessary (e.g., spherical for Pierce type guns). It can be readily mounted on whatever supporting structure is required. While the maximum available emission density is not as high as in the tungsten matrix cathode, which is now used in injected beam CFA's, the work to date shows that enough emission density may be achieved for the requirements of the low-cost CFA's which are the subject of this program. The manufacturing cost of the Medicus cathode is much less than the tungsten matrix cathode because of the machining and processing steps required by the latter. An additional advantage of the Medicus cathode over the tungsten matrix cathode is greater uniformity of emission.

The structure which was used for Medicus cathodes for CFA's is shown in Figure 20. A base block is made for supporting the emitter, and for confining the heater. Two methods of attaching the emitter to the base block were explored, sintering with added nickel powder and laser welding. The sintering process made a poor bond; the laser welding was quite successful.

Low-cost methods of making the cathode base block were considered. If this is a machined part, whether it is molybdenum (as used with tungsten matrix cathodes) or nickel, much of the cost advantage over tungsten matrix cathodes is lost. It appears possible to make the part from nickel powder, pressing in a mold, then sintering. Vendor cost estimates indicated an initial tooling charge of about \$2000, after which the cost per part in large quantities is less than \$1. A final machine cut or grind necessary to assure mounting surface flatness can be done in large batches. The cost of the latter operation would still be quite small as compared with the cost of machining the whole part.



156-022979

Figure 20. Medicus Type Nickel Matrix Cathode For CFA.

For this program two different types of cathode base blocks were made. A sample block of sintered nickel material was obtained from the prospective vendor of sintered nickel parts; cathode base blocks were machined from this. As a back-up, molybdenum base blocks with potted heaters were procured from the vendor of tungsten matrix cathodes; these were like the cathode-heater assemblies used in the first phase of this program except that the impregnated tungsten matrix was omitted. Because of delays by the supplier of heater coils, it was necessary to use the molybdenum block with potted heater.

The second tube model with simulated shaped-substrate meander line was rebuilt with a Medicus cathode like that shown in Figure 20. A new gun assembly fixture was made to assure correct grid location. The gun assembly was mounted in a glass envelope which was evacuated, to determine the heater power necessary for the correct temperature of the Medicus cathode for CFA operation (900 to 950°C brightness temperature).

After the tube was exhausted, emission was very poor. The emitter had evidently become contaminated. The maximum output power which could be achieved was 1.67 kW with 1.2 A beam current.

Since the results achieved in this tube were not definitive, it is of interest to summarize briefly here the results achieved on another program.\* A Medicus type cathode, made in the same way (Figure 20), was mounted in a standard production S-Band CFA. The maximum beam current was 1.3 A peak at 930°C cathode temperature. This represented the temperature-limited condition. For higher temperatures the current fell rather than increasing. Performance of the CFA with this and other values of beam current was not distinguishable from that of the same CFA with a tungsten matrix cathode operating under the same conditions. Tests were made at a temperature of 900°C and beam current of 0.9 A peak. It was observed that the current drooped by about 10%, more or less linearly with time, over a 100  $\mu$ sec pulse. The amount of droop was independent of duty factor when the repetition rate was varied.

\*Contract No. F33615-76-C-1022, Air Force Avionics Laboratory.

When undertaking to apply these results for emission density to the CFA with a shaped-substrate meander line in S-Band, it must be considered that such a CFA has a cathode area 36% greater than the production CFA's because the line is wider. For the same current density, a peak current of 1.3 A in the production CFA's scales to 1.77 A. This is not a comfortable margin for a CFA designed for 1.5 A, but the results suggest that further work on the Medicus cathode is worthwhile for the present application.

## 5. CONCLUSIONS

The first model of the tube with the simulated shaped-substrate meander line clearly showed the feasibility of this type of rf circuit. Efficiency of up to 36% was demonstrated, with power output of 3 kW over much of the 2-4 GHz band. Power output of more than 4 kW was achieved with increased beam current, and efficient operating conditions for 1 kW and 2 kW output were demonstrated. Some minor design changes should lead to significant improvements in performance. The fact that efficiency was continuing to increase with increasing cathode-to-line voltage suggests that the gun position should be modified to produce highest efficiency with lower voltage and higher current (input DC power held constant). The result would be higher gain and greater instantaneous bandwidth. Increased gain is important, since it was observed that increasing the rf drive power leads to increased power and efficiency. It has been estimated that for the operating conditions of these tests, an additional 10 bars (0.480") of line length would be desirable to increase gain sufficiently.

It was shown by cold tests that the ECOM-developed ladder-shaped substrate with a meander line is not significantly different from a meander-shaped substrate in electrical characteristics.

Although power output and efficiency of the CFA with a flat-substrate meander line were not as good as with a shaped-substrate meander line, the flat substrate may still be of interest for some applications, such as in expendable transmitters. The cold-test model indicated the possibility of greater bandwidth than had been supposed. At least part of the deficient performance of the operating model with a simulated flat substrate can be attributed to the fact that the capacitance from line to ground in the cold-test model was not accurately reproduced in the operating model. The conduction from line to ground which appeared after operation could not occur in an actual flat substrate model. The possibility of bar-to-bar conduction which might build up after a period of time would not be of great concern in the special application of expendables, and the lower cost would be of interest.

The Medicus nickel matrix cathode appears to be working close to its present limit in CFA applications. It is not as impervious to mishandling (i.e., poor vacuum, contamination, etc) as the tungsten matrix cathode. It has been demonstrated that the laser welding technique makes it easy to construct cathode assemblies in geometries suitable for CFA's. With better understanding of such cathodes in the future, they may prove quite attractive for CFA's.

## 6. RECOMMENDATIONS

Further work on the shaped-substrate meander line should now go beyond the stage of simulated operating models, and proceed to actual embodiments of this configuration. Interim experimental tubes may still be made using production tube parts extensively elsewhere than for the line, but a total low-cost structure should begin to be considered. Future tube designs require further design calculations of the gun, and of the interaction space based on large-signal theory. Recent experience not only from the present program but also from other R & D efforts should be brought to bear. For example, an optics modification in a recent study by Northrop for the Air Force Avionics Laboratory led to an increase in gain of 5 dB while still maintaining stability.\* In the same study, an analysis of spurious signals of the type which predominated in the data shown in Figure 14 indicates that they may be reduced by a modification of the shape of the bends of the line to reduce electrical discontinuities. Such a modification could be easily introduced into the shaped-substrate meander line.

The flat-substrate meander line should not be abandoned merely on the basis of sub-standard results on one tube model, since the reasons for the deficiencies of that model are understood at least in part. Some previous work on flat-substrate meander lines for X-Band\*\* was also disappointing, but here also the capacitance line-to-ground was too low, and in addition the photo-etched line was not uniform enough. Improved technology now possible should improve this. This approach still has interesting possibilities, for example expendable applications, and for frequency ranges in which the shaped substrate is unduly difficult to fabricate. Any further work on flat-substrate meander lines should be done with actual flat substrates, rather than simulated flat substrates.

\*Contract No. AF33615-75-C-1098.

\*\*Contract No. N0bsr 89504, performed by Warnecke Electron Tubes Inc. (now Northrop) and CSF for Naval Electronics Systems Command.

Because of its potential for low cost and improved performance the Medicus cathode is being pursued by Northrop on other development programs. The base block made of sintered nickel should be tested as a method of cost reduction.

In general, while performance of CFA's has been upgraded and reliability and manufacturability have improved over the past several years, cost reduction has been inhibited because of the modest production quantities required. The approaches described here represent some steps which are needed to bring costs down for larger production quantities.

## BIBLIOGRAPHY

1. J. Arnaud, "General Properties of Periodic Structures", Crossed-Field Microwave Devices (E. Okress, ed.), v.1, p.29, Academic Press, New York (1961).
2. A. Leblond, G. Mourier, "Etude de Lignes a Barreaux a Structure Periodique Pour Tubes Electronique UHF", Ann. Radioelect., v.9, p.318, (1954).
3. R.W. Gould, "Space Charge Effects In Beam Type Magnetrons", J. Appl Phys., v.28, pp 599-605 (1957).
4. W. Sobotka, "Computation of Nonreentrant CFA Characteristics", IEEE Transactions on Electron Devices, v.ED-17, pp 622-632. Aug 1970.
5. G. Dohler, "Beam Injection Control in Broad Band Injected-Beam Crossed-Field Amplifiers", Technical Digest, 1974 Electron Devices Meeting, IEEE, pp 201-204.

DISTRIBUTION LIST  
CONTRACT DAAB07-75-C-1343

<u>ADDRESS</u>	<u>NO. OF COPIES</u>
Defense Documentation Center ATTN: DDC-TCA Cameron Station (Bldg 5) Alexandria, VA 22314	12
Defense Communications Agency Technical Library Center Code 205 Washington, DC 20305	1
Director National Security Agency ATTN: TDL Fort George G. Meade, MD 20755	1
Director, Defense Nuclear Agency ATTN: Technical Library Washington, DC 20305	1
Code R121A. Tech Library DCA/Defense Comm Engring Ctr 1860 Wiehle Ave Reston, VA 22090	1
Office of Naval Research Code 427 Arlington, VA 22217	1
Director Naval Research Laboratory ATTN: Code 2627 Washington, DC 20375	1
Commander Naval Electronics Lab Center ATTN: Library San Diego, CA 92152	1
Commander US Naval Ordnance Laboratory ATTN: Technical Library White Oak, Silver Sprg, MD 20910	1

<u>ADDRESS</u>	<u>NO. OF COPIES</u>
HQ, US Marine Corps ATTN: Code INTS Washington, DC 20380	1
Rome Air Development Center ATTN: Documents Library (TILD) Griffiss AFB, NY 13441	1
Air Force Cambridge Research Lab L.G. Hanscom Field ATTN: LIR Bedford, MA 01730	1
Armament Development & Test Ctr ATTN: DLOSL, Tech Library Eglin AFB, FL 32542	1
HQ, Air Force Systems Command ATTN: DLCA Andrews AFB Washington, DC 20331	1
Director Air University Library ATTN: AUL/LSE-64-285 Maxwell AFB, AL 36112	1
Air Force Systems Command Advanced Systems Div (ASD/ENAD) Wright-Patterson AFB, OH 45433	1
OSASS-RD Washington, DC 20310	1
HQDA (DARD-ARS-P/Drv. R.B.Watson) Washington, DC 20310	1
Commander, DARCOM ATTN: DRCDE-D 5001 Eisenhower Ave Alexandria, VA 22333	1
CDR, US Army Missile Command Redstone Scientific Info Ctr ATTN: Chief, Document Section Redstone Arsenal, AL 35809	2

<u>ADDRESS</u>	<u>NO. OF COPIES</u>
Commander US Army Logistics Center ATTN: ATCL-MA Fort Lee, VA 23801	1
Cdr, Harry Diamond Laboratories ATTN: Library 2800 Power Mill Road Adelphi, MD 20783	1
Commander HQ, Fort Huachuca ATTN: Technical Reference Div Fort Huachuca, AZ 85613	2
Commander US Army Communications Command ATTN: ACC-FD-M Fort Huachuca, AZ 85613	1
Cdr, US Army Research Office ATTN: DRXRO-IP PO Box 12211 Research Triangle Park, NC 27709	1
US Army Security Agency ATTN: IARD Arlington Hall Station Arlington, VA 22212	1
Commander US Army Nuclear Agency Fort Bliss, TX 79916	1
Project Manager, NAVCON ATTN: DRCPM-NC-TM (T.Daniels) Bldg 2539 Fort Monmouth, NJ 07703	1
Commander US Army Satellite Comm Agency ATTN: DRCPM-SC-3 Fort Monmouth, NJ 07703	1
TRI-TAC Office ATTN: CSS (Dr. Pritchard) Fort Monmouth, NJ 07703	1

<u>ADDRESS</u>	<u>NO. OF COPIES</u>
Director, Night Vision Laboratory US Army Electronics Command ATTN: DRSEL-NV-D Fort Belvoir, VA 22060	1
Chief Ofc of Missile Electronic Warfare Electronic Warfare Lab, ECOM White Sands Missile Range, NM 88002	2
Chief Intel Materiel Dev & Support Ofc Electronic Warfare Lab, ECOM Fort Meade, MD 20755	1
Commander US Army Electronics Command Fort Monmouth, NJ 07703	0
DRSEL-PL-ST	1
DRSEL-NL-D	1
DRSEL-WL-D	1
DRSEL-VL-D	1
DRSEL-CT-D	3
DRSEL-BL-D	1
DRSEL-TL-DT (Mr. J.Teti)	1
DRSEL-TL-BM (Mr. C.Bates)	16
DRSEL-TL-BM (Ofc of Record)	1
DRSEL-TE	1
DRSEL-MA-MP	1
DRSEL-MS-TI	2
DRSEL-GG-TD	1
DRSEL-PP-I-PI (Mr. S.Sokolove)	1
DRSEL-GS-H	1
DRSEL-CG	1
DRSEL-PA	2
USMC-LNO	1
DRSEL-RD	1
TRADOC-LNO	1
DRSEL-TL-D	1
DRSEL-TL-B (Mr. I.Reingold)	1
DRSEL-TL-BM (Mr. N.Wilson)	1
DRSEL-TL-BS (Mr. G.Taylor)	1
DRSEL-TL-BG (Mr. S.Scheinder)	1
DRSEL-TL-DS (Mr. B.Reich)	1
DRSEL-WL-A (Mr. M.Adler)	1

<u>ADDRESS</u>	<u>NO. OF COPIES</u>
MIT - Lincoln Laboratory ATTN: Library - Rm A-082 POB 73 Lexington, MA 02173	1
NASA Scientific & Tech Info Facility ATTN: Acquisitions Branch (S-AK/DL) PO Box 33 College Park, MD 20740	2
Advisory Group on Electron Devices 201 Varick St, 9th Floor New York, NY 10014	2
Metals and Ceramics Info Center Battelle 505 King Avenue Columbus, OH 43201	1
Reliability Analysis Center Rome Air Development Center ATTN: J.M.Schrampp/RBRM Griffiss AFB, NY 13440	1
DCASMA, Chicago O'Hare Int'l Airport PO Box 66911 Chicago, IL 60666 ATTN: H.Barcikowski DCRI-GCPE	1
General Electric Company Electronics Park Library Bldg Electronics Park ATTN: Yolanda Burke, Doc Librarian Syracuse, NY 13201	1
Hughes Aircraft Co. Mail Station 3255 P.O. Box 3310 ATTN: Mr. Kalson Fullerton, CA 92634	1
Relmag Div., Microwave Associates 1240 Highway One ATTN: Mr. D. Blank Watsonville, CA 95076	1

<u>ADDRESS</u>	<u>NO. OF COPIES</u>
Raytheon Company Microwave and Power Tubes Div Foundry Avenue ATTN: Mr. J. Skowron Waltham, MA 02154	1
Varian Eastern Tube Div Salem Road ATTN: Dr. G. Farney Beverly, MA 01915	1
Varian Eastern Tube Div Salem Road ATTN: H. McDowell Beverly, MA 01915	1
Litton Industries 1035 Westminster Dr. ATTN: Mr. J. Munger Williamsport, PA 17701	1
Ballistic Missile Defense Advanced Technology Center P.O. Box 1500 ATTN: RDMH-D (D. Schenk) Huntsville, AL 35807	1
Naval Electronic Laboratory Ctr 271 Catalina Blvd ATTN: J. H. Maynard, Code 2300 San Diego, CA 92152	1
Commander, AFAL ATTN: AFAL/DHM, Mr. W. Fritz Wright-Patterson AFB, OH 45433	1
Litton Industries 960 Industrial Road ATTN: Dr. J. R. M. Vaughan San Carlos, CA 94070	1
Microwave Associates South Avenue ATTN: Dr. J. Saloom Burlington, MA 01803	1

ADDRESS

NO. OF  
COPIES

Watkins-Johnson Co.  
3333M Hillview Ave  
Palo Alto, CA 94304

1

ITT Electron Tube Div  
P.O. Box 100  
Easton, PA 18042

1